Post precipitation treatment of copper sulphide particles to improve settleability

By Moses Kumbirai Nduna

Dissertation in fulfillment of the requirements for the degree of Master of Science in Engineering

Department of Chemical Engineering
Faculty of Engineering and the Built Environment
University of Cape Town

3/1/2013

Declaration: I know the meaning of plagiarism and declare that all the work in this document, save for that which is properly acknowledged, is my own.

……

Acknowledgements

I would like to acknowledge my supervisor, Prof Alison Emslie Lewis for her guidance in carrying out this research project. Her leadership was exceptional, while her smile and constant assurance always made the challenges of this research manageable. To my co-supervisor Prof Patrice Nortier, I thank you for making me the researcher I have become. During the course of my stay at UCT, we have exchanged enough emails to last a life time and that is testament to how you were always willing and available to assist.

Many thanks also go to the CPU research officer, Marcos Rodriguez-Pascual, the passion in you to see something positive come out of my research was always evident. Appreciation is also expressed to Ms Christine Olsen, Dr Tracy Craig and Dr Dyllon Randall for making UCT feel like a home away from home.

To all the former and current CPU colleagues, I would like to say thank you for all your support and encouragement. Our endless debates that spanned all the spheres of life never cultivated a dull moment. To all in the Chemical Engineering Department, I am grateful for the opportunity of being amongst you, I am definitely convinced that it is great to be here.

With this work, I hope I have failed my family one less many times. To my mother, my father, my sisters, my brother and little E, thank you for your encouragement, financial and moral support. My friends, Chi(va)^3, Nobert, Michael and Nathan, you are the greatest, may your fortunes be kind to you.

And last but not least, appreciation is given to the WRC for partly funding this work.

Abstract

Surface properties of metal sulphides have a great significance in various areas of engineering and science, such as acid mine drainage, contaminant sorption and metals separation. In various attempts at producing metal sulphide particles from synthetic solutions, prodigious quantities of nuclei which grow only to colloidal dimensions have been frequently reported. This copious nucleation is promoted by high levels of supersaturation which characterises most precipitation reactions. Colloidal particle formation in precipitation-based separation processes results in sub-optimal solid-liquid separation that can be alleviated by the production of more crystalline particles or agglomerates. In order to enhance agglomeration and settling, investigations on the effect of dissolved lattice ions on settleability were performed. This involved suspending precipitated CuS particles in solutions of incremental copper and sulphide ions and measuring the associated settleability. In addition, the effect of partially oxidising precipitated CuS particles with respect to metal ion dissolution, zeta potential and settling was investigated. The experiments were conducted in a 1 L bubble column with oxygen as the oxidising agent. Controlled oxidation was achieved by operating a sparged vessel in incremental residence times. Zeta potential versus pH curves were used as a quantitative measure of the extent of oxidation. Settleability, which gives the volume of settled solids in a litre of suspension within an hour, was used as a measure of settling properties. Improved settleability, by a factor of up to 3, was observed for CuS particles suspended in Cu^{2+} ions, while settleability for particles suspended in S^{2-} ions was completely inhibited. With an increase in oxidation, the concentration of dissolved metal ions increased by a factor of 2 due to dissolution while settling was enhanced by a factor of up to 3.8. The experimentally generated ζ-pH curves of the CuS particles, before and after oxidation, were fitted to a modified CD-Music based surface complexation model in order to try and obtain greater insight into the nature of the respective particles. Analysis of these results suggested substitution of surface thiol groups by hydroxyls with increased oxidation.

Table of contents

Table of contents

Table of contents

Table of figures

Table of figures

List of tables

Nomenclature

a	activity (mol/dm^3)
A	sphere particle radius (m)
a^*	activity at equilibrium (mol/dm^3)
A_H	Hamaker constant (J)
C	concentration (mol/dm^3)
c	number of ions per m^3
D	dielectric constant
e	elementary charge (C)
E	electric field (V/m)
G	Gibbs energy (J)
H	shortest distance between two stern layers (m)
k	boltzmann's constant (J/molecule.K)
k_d	mass transfer coefficient
k_r	reaction rate constant
K_{sp}	solubility product
$\dot{m}$	mass flux (kg/m^2.s)
N_A	Avogadro's constant (mol^{-1})
pH_{iep}	iso-electric point
R	universal gas constant (J/mol.K)
S	supersaturation
T	temperature (kelvin)
V_R, V_A	interaction energy, repulsion and attraction
z	valence
κa	ratio (radius of curvature to double layer thickness for a particle)
k	inverse Debye length (m^{-1})

Nomenclature

Greek symbols

ρ	net charge density (C/m^3)
σ	surface area (m^2)
ψ	electrical potential (V)
γ	interfacial energy (J)
ζ	zeta potential (V)
η	viscosity (Pa/s)
ε	permittivity of medium
μ	chemical potential (J/mol)
μ_E	electrophoretic mobility ($m^2.V.s$)
ν_L	electrophoretic velocity (m/s)

1 Introduction

1.1 Background

Acid Mine Drainage (AMD) in the mining industry is generated when sulphur bearing minerals become exposed and oxidise to form water that has low pH and is high in dissolved metal ion concentration. This phenomenon is mostly prevalent in areas experiencing high mining activity and those that have undergone major earth disturbances. Some metal ions present in AMD are micronutrients for several organisms, but above certain concentrations they become toxic and a danger to natural ecosystems (Sampaio et al., 2010). The conventional method of treating AMD has involved metal hydroxide precipitation. According to Charerntanyarak (1999) and Dyer and co-workers (1998) the minimal hydroxide solubility of some base metals can achieved at an approximate pH range of 9.5-10. This would imply that maximum metal ion removal using metal hydroxide precipitation is at its maximum within this range and any precipitation process done at lower pH levels will compromise metal removal efficiency. Addition of large amounts of lime to attain such high pH levels may lead to increased waste volumes. In most cases the formation of hydroxides is also accompanied by co-precipitation and/or adsorption of various other hydroxide compounds leading to a mixed precipitate (Blais et al., 1999, Marchioretto et al., 2005). Although the formation of mixed precipitates reduces the concentration of total dissolved metal ions it inhibits the selective removal of metal ions.

An approach based on recovery and re-use of metals is not only beneficial to the environment, but may also offer a monetary incentive to companies that are ethically and legally obliged to treat their mining and industrial waste. Sulphide can be a means for the precipitation of a wide variety of metals from solution and offers various advantages over hydroxide precipitation. In metal sulphide precipitation effluent concentrations achieved can be less than 0.01 mg L^{-1} in 1/10 of the volume formed by the alternative conventional hydroxide process (Peters, et al., 1984). Due to the differences in the solubility products of metal sulphides, selective recovery of specific metals may also be possible and this may allow sequential removal of different metals (Veeken & Rulkens, 2003).

Although metal sulphide precipitation has its proven advantages, the widespread application and success of this treatment technology has previously been limited due to the use of expensive chemicals and the potential production of toxic $H_2S_{(g)}$. In an attempt to alleviate such challenges, research in recent years has proposed the use of biogenic sulphide processes. Most heavy metal impregnated wastewaters and AMD are rich in sulphates and bio-processes based on the activity of sulphate reducing bacteria (SRB) offer cost effective reduction of sulphates to sulphide accompanied by the simultaneous precipitation of the metal sulphide species. This results in the removal of both, heavy metal ions and dissolved sulphates. Boonstra and co-workers (1999) successfully showed the applicability of SRBs for the treatment of such waste waters. However, a number of challenges still exist around the precipitation step, particularly aspects concerned with solid-liquid separation. Most work has been focused on optimising sulphate reduction and enhancing microbial activity (Benner, et al., 2002, Kaksonen, et al., 2003, Utgikar, et al., 2002 and Bijmans, et al., 2009) and this has left the subsequent formation of colloidal metal sulphide particles unaddressed. Such particles offer challenges in separating them from the liquid and hence it is necessary to investigate post precipitation techniques that can enhance particle recovery, specifically settleability.

1.2 Scope of Research

Particle rate processes such as nucleation, growth, aggregation, agglomeration and breakage govern particle properties such as particle size distribution (Söhnel & Garside, 1992). Metal sulphide particles in solution develop highly negative surface charge. The magnitude of this charge, if large enough, is responsible for inhibiting aggregation due to particle-particle repulsion. This research is divided into two investigations with the first involving suspending metal sulphide particles into solutions of dilute metal ions or sulphide ions and then observing the respective change in particle settleability. This experiment is accompanied by zeta potential measurements of the metal sulphide particles, before and after modifying the solution chemistry.

It is the aim of the second investigation to subject precipitated metal sulphide particles to partial oxidation treatment in order to modify their surface so as to reduce the magnitude of the negative charge and promote aggregation. However, excessive oxidation of the metal

sulphide particles may result in metal ion dissolution and as such all experiments will be accompanied by dissolved metal ion analysis. The treatment process is carried out post-precipitation when all supersaturation is consumed. Consequently, as small particles aggregate to form larger particles, particle cementation is unlikely, resulting in particle clusters held together by weak van der Waals forces. These clusters may be re-dispersed by conventional particle size measurement techniques because of the high revolutions per minute (rpm) and high hydrodynamic forces subjected to the test suspension as it is pumped and flows through piping and equipment. In order to try and address this challenge, the extent of aggregation was measured in terms of settleability, which involved measuring settling characteristics of precipitated material before and after the proposed treatment.

1.3 Structure of Dissertation

The dissertation is structured into chapters, starting with chapter 1 which introduces the research and sets the project scope. A theory section follows in chapter 2 and it gives a detailed summary of the mechanisms involved in the precipitation process, surface charge development and the subsequent effect of particle charge on suspension stability. A review of the conventional methods employed in minimising colloidal particle formation is given in chapter 3 as well as an overview of the proposed remedial mechanism. After the literature review a combined methodology section follows in chapter 4. This section gives a detailed description of the apparatus, experimental procedure and the analytical techniques used in the study. Chapter 5 details all the obtained results and associated discussions before a concluding section where final conclusions and recommendations are stated. The appendices include raw data, sample calculations and the faculty ethics form.

2 Theory

2.1 Introduction to precipitation

Precipitation generally refers to a relatively rapid crystallisation process characterised by the formation of a sparingly soluble solid phase (Söhnel and Garside, 1992). The rapid kinetics render precipitation processes less susceptible to secondary nucleation caused by the presence of solute material and the characteristic high supersaturation promotes nucleation over growth. This results in a large number of particles with a relatively small size, typically less than 10 µm (Söhnel & Garside, 1992) and (Karpinski & Wey, 2002). The morphology of particles produced during precipitation is thus governed by the extent of secondary processes such as aggregation. In the absence or with inhibition of such processes, precipitation usually results in a colloidal system.

Precipitation in its various forms and configurations has been used in the recovery of dissolved metal ions from industrial waste water and acid mine drainage. The properties (i.e. particle size, morphology and surface area) of formed precipitates are vital in most practical applications and can have major impact on post-precipitation processing, such as solid liquid separation (Söhnel and Garside, 1992).

2.2 Supersaturation

Supersaturation rules the thermodynamic driving force behind all precipitation processes and it is obtained by a chemical reaction that results in the formation of a sparingly soluble product from two soluble reactants. Söhnel and Garside (1992) state that the level of precipitation in a precipitating system governs the particle rate processes, such as nucleation, growth and aggregation. Mersmann (2001), describes supersaturation as the measurement of the difference, $\Delta\mu$, between the chemical potential of the solute in solution, μ, and the chemical potential of the solution in equilibrium with the solid phase, μ^*, as defined by Equation 2.1:

$$\Delta\mu = RT\ln(S) \qquad 2.1$$

$$xA^{z+} + yB^{z-} \leftrightarrow A_xB_y \quad 2.2$$

A typical reaction of precipitation of a solid from dissolved ionic species, represented by Equation 2.2 is decribed at equilibrium by the solubility product as defined by Equation 2.3

$$K_{sp} = (a_A^*)^x.(a_B^*)^y \quad 2.3$$

According to Mersmann (2001) and Söhnel and Garside (1992), supersaturation in aqueous solutions expressed in ion activity is given as shown in Equation 2.4.

$$S = \left(\frac{(a_A)^x(a_B)^y}{K_{sp}}\right)^{\frac{1}{x+y}} \quad 2.4$$

2.3 Particle rate processes

Kinetic processes of nucleation, growth, aggregation and breakage can be defined as particle rate processes and are responsible for the change in particle size distribution with time during precipitation. The processes can act in synergism or antagonism with one another and understanding these complex interactions is crucial in predicting and controlling precipitation.

2.3.1 Nucleation

The formation of the first stable solid (nuclei) in solution can be defined as nucleation (Söhnel and Garside, 1992). The build-up of supersaturation in a solution is a pre-requisite to nucleation and creates the driving force for nuclei formation, either spontaneously or induced. Supersaturation may be derived by a change in temperature, pH, pressure and any appropriate strain to the system. Because of their small size, the creation of these nuclei requires extra free energy associated with the interfacial energy and the creation of surface.

$$\Delta G(i) = -iRT\ln(S) + \gamma.\sigma(i) \quad 2.5$$

The work of formation, $\Delta G(i)$, of a mole of clusters consisting of i molecules from a solution at supersaturation S is given in Equation 2.5, where γ is the interfacial energy between the nucleating phase and the solution and $\sigma(i)$ is the surface area created by the clusters.

Nucleation processes in systems that do not yet contain the precipitating matter are termed 'primary' while nucleation in the presence of the precipitating matter is termed 'secondary'. This is presented in the following scheme:

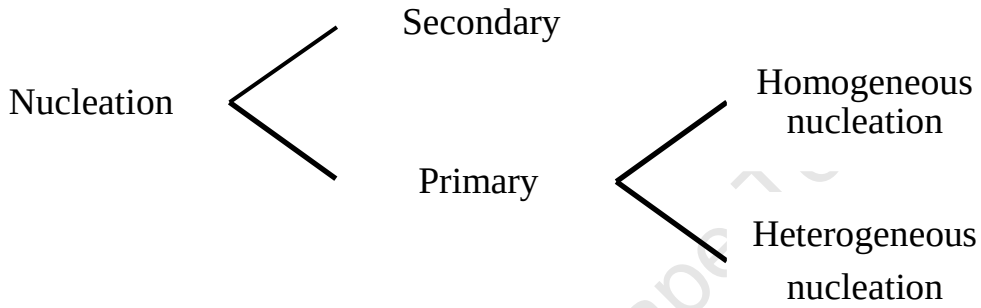

Figure 2.1: Nucleation mechanisms (Mullin, 2001)

Within primary nucleation a further distinction can be made depending on the local conditions around the forming nuclei. Homogenous nucleation results in the formation of a solid phase not initiated by the presence of any solid and heterogeneous nucleation results in the formation of a solid phase catalysed by the presence of a foreign solid phase (Mullin, 2001).

2.3.2 Growth

As soon as nuclei are formed, in the presence of supersaturation, they begin to grow into crystals. Crystal growth is due to two main processes which occur sequentially within a solution. The first is the mass transport of growth units from the bulk solution to the solution-crystal interface by bulk diffusion and the second is the incorporation of the growth units into the crystal lattice through surface integration. The slower of the two steps is the rate determining step and the growth units can be molecules, ions, clusters, monomers, etc.

According to Mullin (1972), these two steps can be further classified into the following distinguishable steps when dealing with crystal growth of an ionizing solute:

1. Bulk diffusion of solvated ions through the diffusion boundary layer
2. Bulk diffusion of solvated ions through the adsorption layer
3. Surface diffusion of solvated or unsolvated ions
4. Partial or total desolvation of ions
5. Integration of ions into the lattice
6. Counter-diffusion through the adsorption layer of the water released
7. Counter-diffusion of water through the boundary layer

The entire concentration gradient which makes the system supersaturated, $\Delta C = C - C^*$, can be divided into two parts. The diffusive-convective layer which causes diffusive-convective transport is the first part, defined by $C - C_I$, whereas $C_I - C^*$ is the second part and is decisive for the integration reaction within a reaction boundary layer. When growth is completely determined by diffusion and convection, such a system is defined by Equation 2.6 (Mullin, 2001) while Equation 2.7 (Mullin, 2001) defines a system completely controlled by the integration step.

$$\frac{C_I - C^*}{C - C_I} \leq 1 \tag{2.6}$$

$$\frac{C - C_I}{C_I - C^*} \leq 1 \tag{2.7}$$

$$\dot{m} = k_d(C - C_I) = k_r(C_I - C^*)^r \tag{2.8}$$

The mass flux density ($\dot{m}$) is given by Equation 2.8 where, I represents conditions at the interface, * represents conditions at equilibrium, k_d is the mass transfer coefficient, k_r is the reaction rate constant, r is the order of integration and C is concentration. Temperature dependence of the reaction rate constant is generally defined by the Arrhenius equation.

2.3.3 Aggregation

Aggregation is the unification of particle clusters without their subsequent cementation by crystal bridges (Mersmann, 1999). Since particle cementation is absent, supersaturation is not a pre-requisite for aggregate formation. The particles are held together by weak cohesive forces such as the van der Waals forces and thus can be more readily destroyed. In some cases aggregation is regarded as the intermediate process preceding agglomeration and succeeding coagulation. Aggregation consists of two steps:

i. The collision of particles, which can be due to a number of mechanisms that include: Brownian motion and/or diffusion, in which case it would be referred to as perikinetic aggregation. With orthokinetic aggregation, the motion of the particles is due to hydrodynamic motions, such as convective currents and mechanical stirring.

ii. The staying together of particles, commonly referred to as the collision efficiency, is governed by the magnitude of repulsive and attractive interactions during a collision. In such cases, altering the solution chemistry and particle surface characteristics, the inter-particle forces may be modified to promote repulsion or attraction. This may induce or prevent the staying together of particles and the latter is termed electrostatic stabilization. For certain systems the shape and orientation of particles may dictate the collision efficiency and in such cases it is termed steric stabilization.

2.3.4 Agglomeration

Agglomeration is dependent on the successful aggregation of particles and involves the cementing together of particles by the formation of inter-particle crystalline bridges (Hartel, et al., 1986). Hence, agglomeration is dependent on kinetic processes that control crystal growth and supersaturation. The formation of crystal bridges between two or more crystals requires growth and consumes supersaturation and hence strong agglomerates are only formed in supersaturated solutions. Agglomeration can result from malgrowth of crystals or from crystal-crystal collisions in supersaturated solutions. At the onset of precipitation, the governing factor appears to be the classical mechanism of ion attachment to nuclei rather than

agglomeration of molecular aggregates or nuclei (Söhnel, et al., 1988). Agglomerates are generally more difficult to disperse than aggregates.

2.4 Particle Surface Charge

A surface or interface exists where there is an abrupt change in system properties with distance. These may include density, crystal structure, etc. Particle surfaces may develop charge as a result of one or more of the following mechanisms (Everett, 1988) and (Hunter, 1986).

i. If in contact with a different phase, charge may arise due to a difference in electron/ion affinity of the two phases.

ii. Ionisation of surface groups:
In cases where the surface contains acidic groups their dissociation gives rise to a negatively charged surface, and conversely a basic surface takes on a positive charge. The magnitude of the surface charge depends on the extent of the respective dissociation.

iii. Isomorphous substitution:
This can be the exchange of an adsorbed, intercalated, or structural ion with one of a lower valency, resulting in a negatively charged surface

iv. Colloid surface defects:
This results from surface bond cleavage/unsatisfied bonds

v. Differential solution of ions from the surface of a sparingly soluble crystal/colloid. When a silver iodide crystal is immersed in water, silver ions preferentially dissolve leaving a negatively charged surface, a result of iodine ions in slight excess.

2.5 Electrical Double Layer

When a charged colloidal particle is immersed in an electrolyte solution, it is surrounded by ions of the opposite sign to balance the surface charge. Various models attempt to address this, but the simplest model of the double layer is attributed to Helmholtz (1879). He envisaged an arrangement of charges in two rigid parallel planes as shown in Figure 2.2:

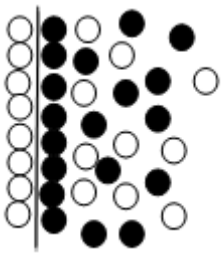

Figure 2.2: Helmholtz model of EDL (Everett, 1988)

The Helmholtz model has however been recognised as an inadequate representation of the double layer because of its inability to account for thermal motion. The surface of a solid can be regarded as having a constant potential, while this is not the case for ions in solution.

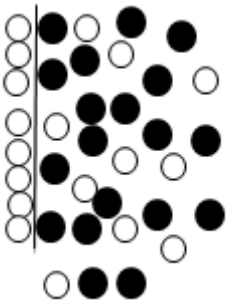

Figure 2.3: EDL model incorporating thermal motion (Everett, 1988)

The Gouy (1910) and Chapman (1913) model, states that the counter-ions are not rigidly held around the colloid surface, but diffuse in to the bulk phase until the counter potential set up by their departure inhibits such movement. A diagram showing the electrical double layer as envisaged by Gouy and Chapman is shown in Figure 2.3. The Gouy-Chapman theory is the basis used in developing the Poisson-Boltzman equation, which has become the conventional theory of describing the ionic distribution and net electrostatic potential of the electrical double layer. If at some point in an electrolyte a charge potential exists, Boltzmann's law indicates that the concentration of positive ions will be defined by Equation 2.9 (Everett, 1988):

$$C_x(+) = C^0\exp(-\frac{z^+e\psi(x)}{kT}) \quad 2.9$$

where $\boldsymbol{z}^+$ is the valence of the positive ion, $C_x(+)$ is the concentration of positive ions at a distance x from the charged surface, C^0 the concentration of positive ions in a region where $\psi=0$ and $\boldsymbol{e}$ the elementary/protonic charge. This follows from the fact that if an ion is next to a charged surface, it must be in equilibrium with the respective ions in the bulk. At a distance x, from a charged surface, the electrochemical potential of an ion should equate to its bulk value. For negative ions the concentration would be defined by Equation 2.10 (Everett, 1988):

$$C_x(-) = C^0\exp(+\frac{z^-e\psi(x)}{kT}) \quad 2.10$$

In this region around the charge centre, an electrical imbalance of charges exists, which in the case of $\boldsymbol{z}^+$ and $\boldsymbol{z}^-$ being equal to z, it would be defined by Equation 2.11 (Everett, 1988).

$$C_x(+) - C_x(-) = C^0[\exp(-\frac{ze\psi(x)}{kT}) - \exp(+\frac{ze\psi(x)}{kT})] \quad 2.11$$

If the region under consideration is close to a positively charged centre, ψ will be positive and $[C(+) - C(-)]$ will be negative. Consequently this means that around a positive ion there will be an excess of negative charge, called a charge cloud or ionic atmosphere. However, the charged particles and the electrolyte solution, as a whole, remain electrically neutral and it is the charge cloud or ionic atmosphere around a charged surface that is called the electrical double layer.

The Gouy-Chapman theory provides a better approximation of the double layer than the Helmholtz model, but still has its limitations. It characterises ions as point charges and assumes no physical limit in ion approach to the surface, which has been found to be unrealistic (Stern, 1924 cited by Stachowicz, et al., 2006). Stern modified the Gouy-Chapman diffuse double layer and stated that ions do have a finite size, so cannot approach a surface

closer than the respective ion radius, a distance he termed δ. He also stated that some ions are specifically adsorbed by the surface in the pane δ, a layer that has become known as the Stern Layer. This means that over the diffuse layer, the potential, ψ, will drop by ψ_δ, a value that has become considered an approximation to the Zeta Potential (ζ), which can be determined by micro-electrophoresis. The distance experiencing ion imbalance around the colloid particle depends on the charge potential of the colloid surface as well as the concentration of ions in the electrolyte. Electrostatic potential and charge density are related by the Poisson's equation, defined as follows:

$$\frac{d^2\psi(x)}{dx^2} = \frac{\rho(x)}{\varepsilon_0 D} \qquad 2.12$$

Where D is the static dielectric constant of the medium and ε_o is the permittivity of free space. This leads to the development of the Poisson-Boltzmann (PB) equation, shown in Equation 2.13 (Shaw, 1970):

$$\frac{d^2\psi(x)}{dx^2} = \frac{2zeC^0}{\varepsilon} sinh \frac{ze\psi}{kT} \qquad 2.13$$

Resolution of the Poisson-Boltzmann equation provides that, for a uniformly distributed charge, the charge density falls exponentially with distance from the surface, as shown in Figure 2.4 and described by Equation 2.14 (Shaw, 1970):

$$\Psi(x) = \psi^0 \exp(-\kappa x) \qquad 2.14$$

Where:

$$1/\kappa = [\varepsilon kT/e^2 \Sigma c_i z_i^2]^{0.5} \qquad 2.15$$

At distance $1/\kappa$ the potential drops by a factor of $1/e$, c_i is the number of ions per m^{-3} and ε is permittivity (Everett, 1988). $1/\kappa$ as defined by Equation 2.15 is termed the "Debye Length" and is the characteristic length of the potential decrease around the particle.

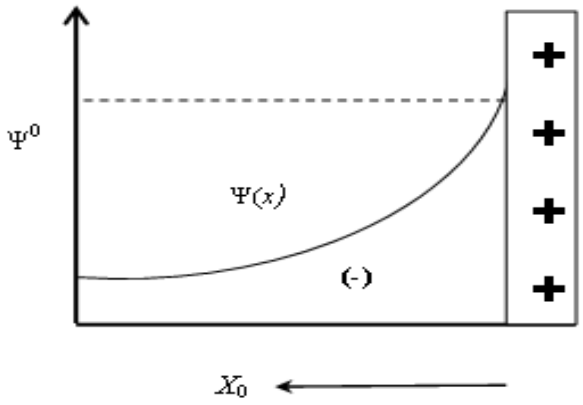

Figure 2.4: Charge potential with distance from particle surface

The significance of this theory is the fact that the thickness of the double layer depends on the ionic concentration of the electrolyte. In the case of a flat surface typical Debye lengths are shown in Figure 2.5, in each case the potential drop is $100/e$ or 37 mV.

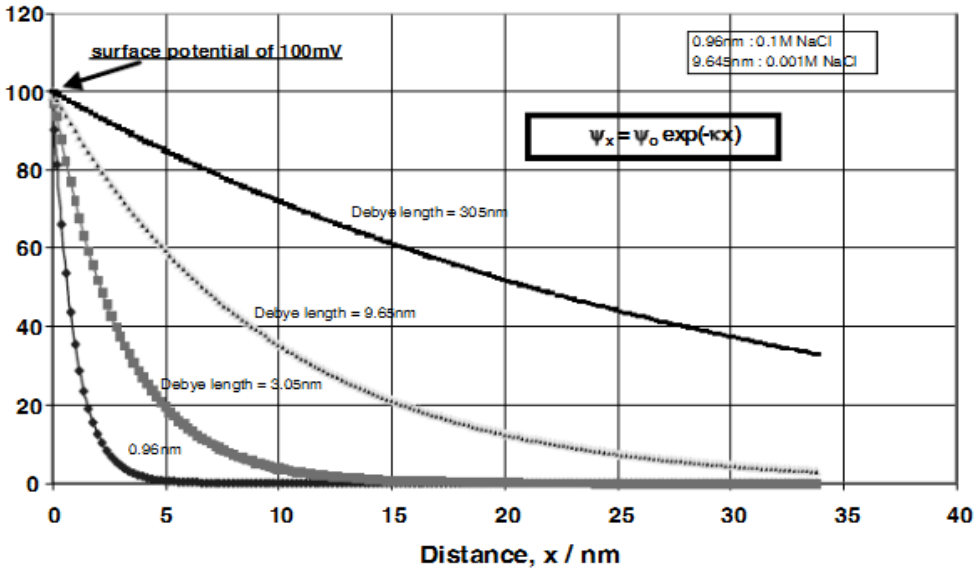

Figure 2.5: Electrostatic potential decay with varying electrolyte strength (Pashley & Karaman, 2004)

2.6 Colloidal Stability

A colloidal dispersion is a heterogeneous system consisting of solid nanoparticles dispersed in a fluid medium. These particles are small enough to undergo Brownian motion, resulting in continuous collisions with one another. The particles remain as single particles as long as the collisions do not result in permanent associations. The ability of the particles to remain as individual particles is termed colloidal stability and the mechanism by which "unstable" colloidal suspensions evolve is aggregation. Colloidal stability can be achieved by several ways, of which the following two are the most classical:

i. The particles can be given a charge, either negative or positive. If all the particles have the same charge they can repel each other to a lesser or greater extent when they approach each other. This is referred to as electrostatic stabilisation.
ii. The particles can be coated with a polymer that always orientates the particles in such a way that when they collide, the excluded volumes of the polymeric shells hinder aggregation. This type of stabilisation is referred to as steric stabilisation.

Deryagin and Landau (1941) and Verwey and Overbeek (1948) independently developed a quantitative theory in which the electrical stability of colloidal dispersions was treated in terms of the energy changes that take place when particles with an electrical double layer approach one another. The theory is based on net interaction energy due to an overlap of electric double layers (repulsion) and van der Waals forces (attraction) in terms of interparticle distance. If the electrical double layer (EDL) of two particles overlap in a typical Brownian motion encounter, Overbeek (1977) states that the rate of overlap is too fast for adsorption equilibrium of EDL ions to be maintained, resulting in a change of particle surface charge. For low surface potential (ψ_0 < 25 mV), the resultant potential energy of repulsion between two colliding particles is given by Equation 2.16 (Everett, 1988):

$$V_R^{\psi} = \frac{\pi \varepsilon A1A2(\psi^2 d1 \psi^2 d2)}{(A1+A2)} \{ \frac{(2\psi d1\ \psi d2)}{(\psi^2 d1 \psi^2 d2)} . ln\left(\frac{1+exp[-\kappa H]}{1-exp[-\kappa H]}\right) + ln(1 - exp[-2\kappa H]) \} \qquad 2.16$$

Where a_1, a_2 relates to the radii of two spherical particles, H is the shortest distance between the stern layers and $\kappa = \left(\frac{2e^2 N_A \mathrm{C}\, \mathrm{z}^2}{\varepsilon \mathrm{k} T}\right)^{0.5}$. For equal spheres ($A_1 = A_2$), Equation 2.16 reduces to Equation 2.17 (Everett, 1988):

$$V_R^{\psi} = 2\pi \mathcal{E} A \psi_d^2 ln(1+exp[-kH] \qquad 2.17$$

For higher potentials and unequal spheres, a more useful approximation is that given by Reerink and Overbeek (1954), and defined by Equation 2.18:

$$V_R = \frac{64\pi \mathcal{E} A^1 A^2 k^1 T^2 \gamma^1 \gamma^2}{(A1+A2) e^2 z^2} exp[-kH] \qquad 2.18$$

And for equal spheres Equation 2.18 reduces to Equation 2.19:

$$V_R = \frac{32\pi \mathcal{E} A^1 A^2 \kappa^1 T^2 \gamma^1 \gamma^2}{e^2 z^2} exp[-\kappa H] \qquad 2.19$$

In the case of van der Waals interactions, the force experienced by two colliding spherical particles of radii A_1 and A_2 is defined as shown in Equation 2.20:

$$V_A = -\frac{A_H}{12}\left[\frac{y}{x^2+xy+x} + \frac{y}{x+xy+x+y} + 2\ln\left(\frac{x^2+xy+x}{x^2+xy+x+y}\right)\right] \qquad 2.20$$

Where the following notation is specific for Equation 2.20: $x = \frac{H}{A_{1+}A_2}$ and $y = \frac{A_1}{A_2}$

For equal spheres Equation 2.20 takes the form defined by Equation 2.21:

$$V_A = -\frac{A_H}{12}\left[\frac{1}{x(x+2)} + \frac{1}{(x+1)^2} + 2\ln\left(\frac{x(x+2)}{(x+1)^2}\right)\right] \qquad 2.21$$

The summation of attractive and repulsive energies that gives the net interaction energy between two colliding particles is shown in Figure 2.6, where net interaction energy is plotted against distance of two colliding particles. A positive potential indicates a dominant repulsive force, whereas a negative potential indicates a dominant attractive force. The primary minimum corresponds to the minimum in the energy curve at the left hand side of the energy barrier while the secondary minimum is usually not sufficiently deep to have practical implications. Electrophoretic mobility, measured by zeta potential, can be used to predict the electrostatic forces experienced by colloidal particles in solution.

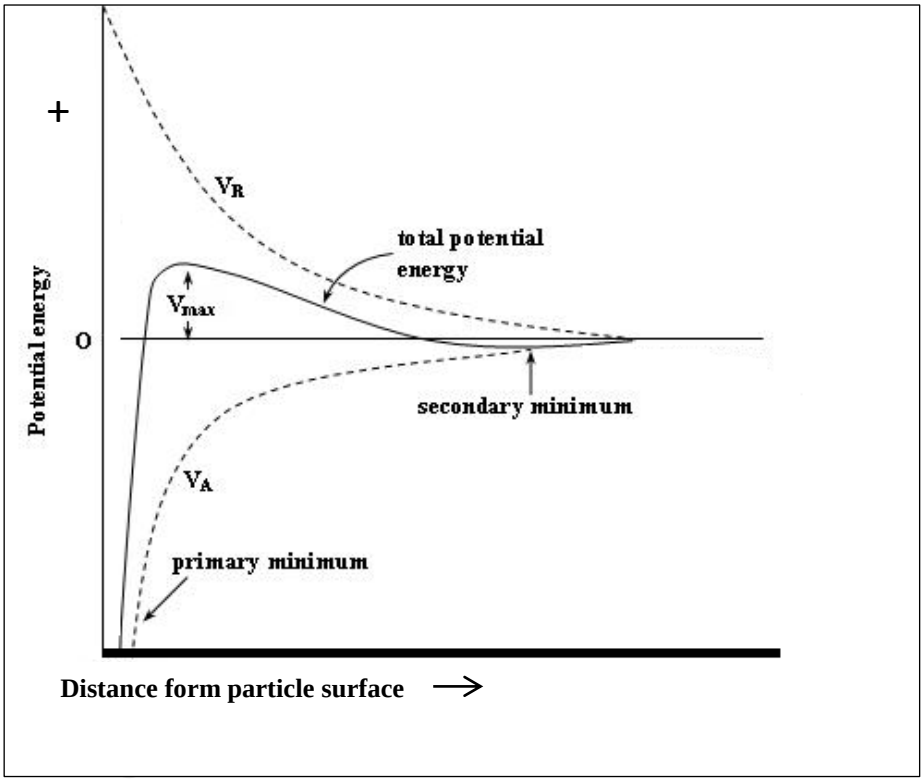

Figure 2.6: The net interaction energy between two colliding particles (Hunter, 1986)

2.7 Electrophoresis

Electrophoresis refers to induced motion of suspended particles in response to an applied electrical field. It follows that an isolated particle carrying a charge in an electric field would experience a force directed towards the oppositely charged electrode as defined by Equation 2.22 where q is the charge of the particle and E is the electric field (Shaw, 1970).

$$F_{el} = qE \quad (2.22)$$

$$v_L = \mu_E E \quad (2.23)$$

The migration rate of the particles is proportional to the applied field strength, the potential at the shear plane and inversely proportional to the viscosity of the medium. The electrophoretic mobility, μ_E, is defined as the ratio of the velocity by the electrical field as defined by Equation 2.23. It is calculated from the applied electric field and the measured velocity and this is used to obtain the zeta potential from the Henry equation, as defined in Equation 2.24:

$$\mu_E = \frac{2\varepsilon\zeta}{3\eta}.f(\kappa a) \quad (2.24)$$

Where ζ is the zeta potential, ε is the permittivity, η is viscosity and $f(\kappa a)$ is the Henry's function. For electrophoretic determinations in aqueous media and moderate electrolyte concentrations (particles < 0.2 μm and concentration < 10^{-3} M) the Henry's function is taken as 1.5. For small particles in media with a low dielectric constant the Henry's function is taken as 1.0 and this usually applies for non-aqueous measurements.

In this study zeta potential is measured via micro-electrophoresis and the technique used to measure the velocity of the suspended particles is referred to as Laser Doppler Velocimetry. A beam of light is passed through a point in a translucent cell containing the study suspension. Some of the light in this beam is scattered at an angle of 17° and upon reaching the receiving optics it is combined with the reference beam. A fluctuating intensity signal is produced where the rate of fluctuation is proportional to the speed of the particles.

3 Literature Review

Various methods have been used on different metal sulphide systems to try and reduce the particle electrostatic repulsion (zeta potential) in order to induce settling. The methods involved include the control of supersaturation to produce non colloidal particles, by promotion of growth and secondary nucleation (Sampaio, et al., 2010), as well as the use of additives which may promote coagulation (Mokone, et al., 2012).

3.1 Supersaturation

It has become generally accepted that the prerequisite for the production of non-colloidal sulphide particles is to operate under mildly supersaturated conditions (van Hille, et al., 2005 and Jones, et al., 1996). Several mechanisms to control supersaturation have been proposed. Lewis (2006) employed multiple reagent feed points in a fluidised bed reactor in order to spread supersaturation and produced a reduced amount of cobalt and nickel sulphide fines. This method was however less successful when adopted by Mokone and co-workers (2012) in a seeded fluidised bed reactor, varying between 2 and 6 reagent feed points. During the precipitation of CuS and ZnS they found that using an increased number of reagent feed points did not significantly reduce the number of fines produced during the precipitation process although it altered the surface structure of the precipitated particles, without affecting the settling characteristics. This could imply that increased feed points do not have the same overall effect on all metal sulphide systems. Further to this, van Hille and co-workers (2005) observed a significant amount of fines at the point of sulphide injection in a fluidised bed reactor. Taking this into account, it is possible to assume that increasing the number of feed points would result in an increase in the source of fines and therefore may actually be counterproductive for some systems. This remains to be fully explored but will not be dealt with in this study.

According to Schlauch (1978), non-colloidal metal sulphide particles can be formed by controlled sulphide release into a solution containing pollutant metal ions. He proposed the

addition of a metal sulphide slurry, such as FeS, having a higher solubility into a stream containing metal ions, such as Cu^{2+} ions, with a much lower metal sulphide solubility. When the FeS slurry is added to the Cu^{2+} metal ion stream it attains equilibrium according to Equation 3.1 and is governed by the equilibrium solubility product. Due to a much lower solubility product of CuS, all available S^{2-} ions react with Cu^{2+} ions according to Equation 3.2 and precipitate CuS. As Equation 3.2 consumes S^{2-} ions, the equilibrium of Equation 3.1 shifts to the right resulting in further dissolution of FeS into its constituent ions. The process of CuS precipitation thus becomes controlled by the dissolution of FeS, which is dependent on pH, temperature and solids concentration. Although this process may seem viable it depends greatly on the ability to isolate a pure metal sulphide, to be used as a sulphide ion source.

$$FeS_{(s)} \leftrightarrow Fe^{2+}_{(aq)} + S^{2-}_{(aq)} \quad 3.1$$

$$Cu^{2+}_{(aq)} + S^{2-}_{(aq)} \leftrightarrow CuS_{(s)} \quad 3.2$$

Hammack and co-workers (1993) successfully exploited the pH dependence of sulphide speciation in controlling supersaturation. They operated a hydrogen sulphide-based precipitation process under acidic conditions. This reduced the rate of $H_2S_{(g)}$ dissolution, thereby reducing the equilibrium concentration of the HS^- ion in solution resulting in a decrease in the effective supersaturation. A notable decrease in the amount of fines produced was reportedly observed. The equilibrium relationship that exists between the species: $H_2S_{(aq)}$, HS^- and S^{2-} is as defined by Figure 3.1. Karbanee and co-workers (2008) also exploited mass transfer resistance, from the dissolution of sparged $H_2S(g)$, to control sulphide dosing. Although the method managed to successfully control sulphide ion dosing, the process was compromised by the production of H^+ ions as a result of H_2S decomposition as defined in Equations 3.3 and 3.4:

$$H_2S_{(aq)} \leftrightarrow HS^-_{(aq)} + H^+_{(aq)} \quad 3.3$$

$$HS^-_{(aq)} + H^+_{(aq)} \leftrightarrow S^{2-}_{(aq)} + 2H^+_{(aq)} \quad 3.4$$

The hydrogen ions lowered the pH to levels that promoted the dominant speciation of $H_2S_{(aq)}$ in solution over that of the HS^- and S^{2-} ions as shown in Figure 3.1. To prevent the exhaustion of the HS^- ion in solution, NaOH had to be continually added as a pH modifier to raise the pH and maintain optimal HS^- speciation. As well as a cost implication associated with the need for additional pH controlling reagents, the use of $H_2S_{(g)}$ has significant health and safety challenges due to the toxicity of the gas involved.

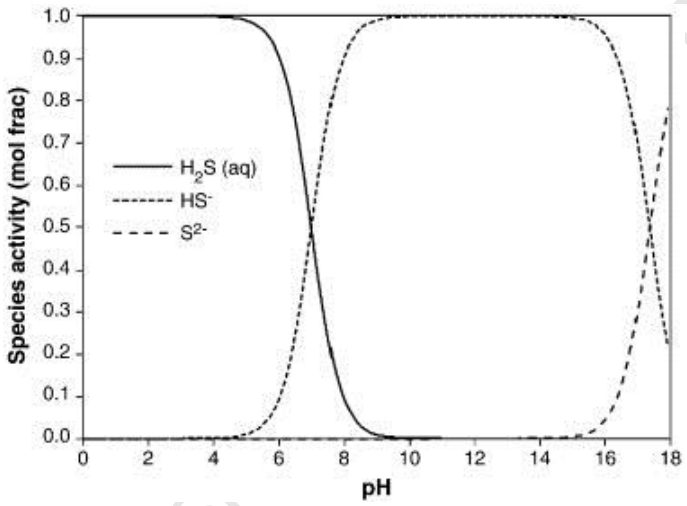

Figure 3.1: pH dependence of hydrogen sulphide speciation (Lewis, 2010)

In trying to alleviate challenges associated with having regions of high supersaturation at the point of gas injection in a H_2S based precipitation process, Bijimans and co-workers (2009) proposed the use of a sulphate reducing bioreactor (SRB) with the SRB cells acting as well dispersed sulphide injection points. In further work by Veeken and co-workers (2003) they noted that creating a system of homogenous supersaturation was necessary in producing non-colloidal particles. They employed controlled sulphide dosing using a sulphide specific probe and created a high specific area with a membrane precipitator reactor leading to the production of non-colloidal ZnS particles.

Although the proposed methods maybe practical and successful to varying extents for different metal sulphide systems, some are very complex to manage on a large scale and may require intensive process control. In cases where the control of supersaturation remains a challenge it may be necessary to consider other options of promoting non-colloidal particle formation or aggregation.

3.2 Solution chemistry

3.2.1 Addition of excess precipitating ions

According to Ottewill (1982), depending on the solution chemistry, electrostatic repulsive forces are inhibited and do not restrict aggregation within a zeta potential range of -15 mV to +15 mV. The variations within this range may depend on the Hamaker constant which varies for the different metal sulphides. Vergouw and co-workers (1998i) showed that the maximum settling velocity for PbS and FeS was observed roughly coincident with the respective IEP as shown in Figure 3.2 and Figure 3.3 respectively. This suggests that a correlation exits between the maximum aggregation and the iso-electric point and as such may lead to the conclusion that metal sulphide suspensions obey the DLVO theory. This is also consistent with a rheological study performed on synthetic sphalerite suspensions, where the largest yield stress was noted at the iso-electric point (Muster & Prestidge, 1995).

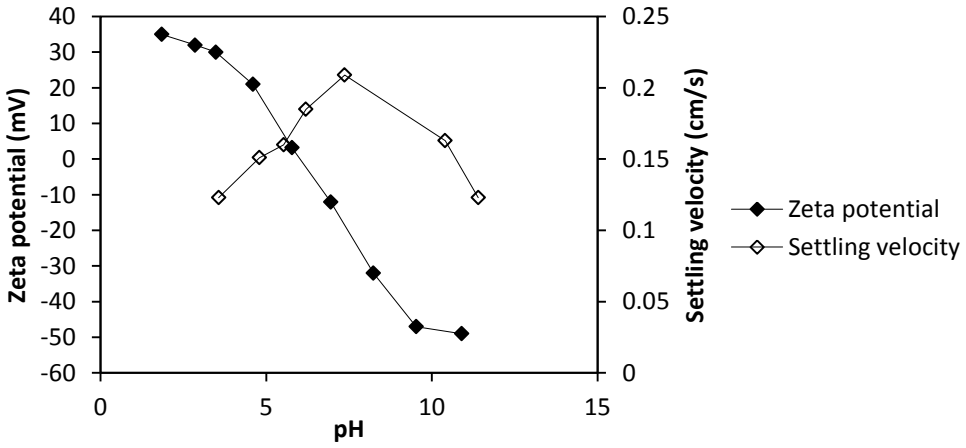

Figure 3.2: Comparison between zeta potential and settling rates of Pyrite (Vergouw *et al*., 1998i)

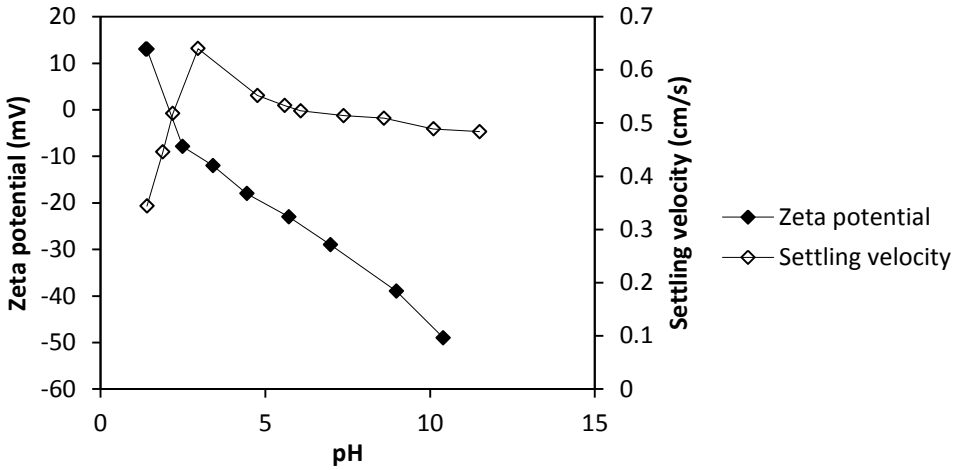

Figure 3.3: Comparison between zeta potential and settling rates of Galena (Vergouw *et al*., 1998i)

However, contrary to the anticipated behaviour, DiFeo and co-workers (2001) observed an increase in settling rate with an increase in the magnitude of the zeta potential. In a ZnS system with an iso-electric point of 3.5, they observed the maximum settling rate at a pH of 8.5, 5 pH units from the isoelectric point, corresponding to a zeta potential of about -27 mV. This is also consistent with work by Vergouw and co-workers (1998ii) on ZnS, who observed the highest settling at a pH of around 10 and a zeta potential of -40 mV. They suggested that the unexpected particle stability at high zeta potentials was as a result of the existence of a hydrophobic force on the particles surface sufficient to overcome electrostatic repulsion. Although a contact angle study confirmed the hydrophobic nature of the surface, the exact nature of the species was not stated. This is consistent with a growing notion in literature that not all colloidal solutions are governed by the classical DLVO theory and hence considering the van der Waals and electrostatic forces (zeta potential) is not a sufficient measure to describe colloidal stability (Grasso *et al*., 2002). However, in settling investigations it may not be imperative to account for all non-DLVO forces, but rather to understand that the iso-electric point does not necessarily translate to maximum aggregation and hence settling.

Mokone and co-workers (2010) explored changes in the solution chemistry as a means of reducing zeta potential. In that study, the metal to sulphide ratio was varied between 0.67, 1

and 2, representing a solution deficient in metal ions, equi-molar in metal to sulphide ions and excess in metal ions respectively.

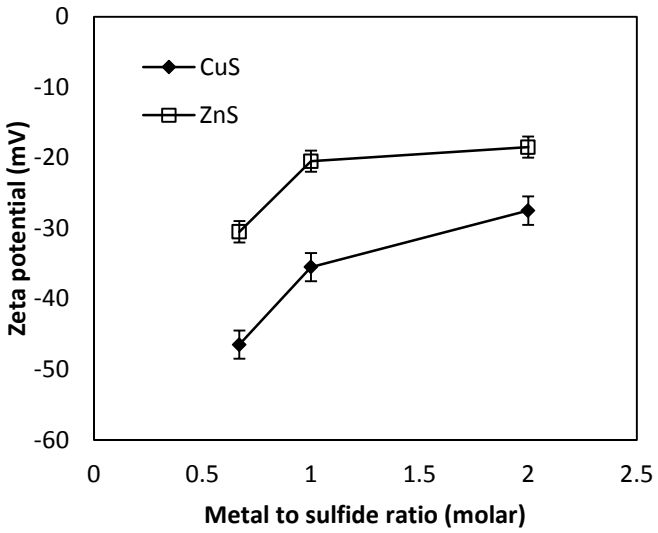

Figure 3.4: Effect of metal to sulphide ratio on zeta potential (Mokone *et al*., 2010)

As shown in Figure 3.4, the zeta potential of both ZnS and CuS increased (became less negative) from -20.5 and -35.5 mV for equimolar concentrations to -18.5 and -27.5 mV respectively at a metal to sulphide ratio of 2. Mokone and co-workers (2010) noted that the decrease in the zeta potential of ZnS did not translate to improved aggregation. This could be attributed to the fact that, although the respective zeta potential increased (became less negative), it was still below the threshold value of -15 mV above which aggregation would be promoted. For the CuS system, they noted that the increase in the zeta potential upon changing the metal to sulphide ratio from 1 to 2 did not translate to a change in the particle size distribution, hence very little change in the agglomeration properties of the system. However, they observed that agglomeration was greatly reduced when the zeta potential of the sulphide particles decreased to about -46.5 mV at a metal to sulphide ratio of 0.67. This suggests that in addition to having a lower zeta potential magnitude limit, below which aggregation is promoted, a metal sulphide suspension may also have an upper zeta potential magnitude limit at which aggregation is predominantly inhibited.

It may be reasonable to assume that, with a further increase in the metal to sulphide ratio, the method used by Mokone and co-workers (2010) could yield metal sulphide particles with a zeta potential within the range of -15 to +15 mV. This, however, could be detrimental to the actual cause in which metal sulphide precipitation is employed to eradicate. If metal sulphide precipitation is used to scavenge metal ions from acid mine drainage or industrial waste, it would then be self-defeating to have the metal ions in excess by at least 200%. van Hille and co-workers (2005) also noted that large deviations from equimolar precipitating conditions resulted in changes in the morphology of the precipitating particles and that this may compromise the quality of the particles. Under certain conditions as well, the excess ions may precipitate secondary species such as hydroxides and this may create challenges in multiple solids separation. Thus the use of much lower concentrations on specific metal sulphide systems would need to be investigated.

The effect of excess metal ions in more moderate quantities has also been investigated by various authors. In a study conducted by Vergouw and co-workers (1998), the zeta potential and settling characteristics of FeS and PbS suspended in indifferent electrolytes were compared to those when the two metal sulphide systems were suspended in 15 ppm electrolyte solutions of the respective metal ions. Upon the dispersion of PbS particles in to a 15 ppm solution of Pb^{2+} ions, the zeta potential versus pH behaviour of the particles changed from having one iso-electric point at a pH of about 2, in an indifferent electrolyte, to having 3 iso-electric points at pH values of 2.8, 4.2 and 6.8. It was also noted that the highest settling rates were observed around the stated iso-electric points. Contrary to expectations however, the particle settling rate was observed to increase at high pH values beyond the third iso-electric point as the zeta potential became more negative. According to the authors, the reason for such behaviour remains unclear. In the case of FeS, suspending the particles in a 15 ppm Fe^{2+} ion suspension increased the isoelectric point from a pH of 6.2, in an indifferent electrolyte, to a pH of 7 but no multiple charge reversal was observed. The addition of Fe^{2+} ions led to a general decrease in settling rate over the investigated pH range from pH 4 to pH 12 and there was no strong correlation between the iso-electric point and the maximum settling rate. On the other hand however, Bebie and co-workers (1998) observed an increase in zeta potential and multiple charge reversal upon addition of FeS particles to a solution of about 28 ppm Fe^{2+} ions. It is tempting to attribute the variance on the effect of Fe^{2+} ions from one system to another on the difference in concentration, 15 ppm and 28 ppm, but this would

have to be verified by experimental analysis. The difference in the effect of Pb^{2+} ions and Fe^{2+} ions on the stability of their respective metal sulphide systems means that the effect of metal ions on colloid suspensions cannot be generalised and applied in a broad sense to all metal sulphide systems.

3.2.2 Effect of ionic strength

Söhnel and Garside (1992) stated that, with an increase in ionic strength: (a) due to mono- or bivalent ions, the zeta potential of particles may approach zero through a maximum, (b) due to bi- or trivalent ions, the zeta potential may fall towards zero and (c) in the presence of tri- and tetravalent ions, the zeta potential may fall to a minimum below zero then with further ion addition it may increase again towards zero. This theory, however, remains generally untested for the full spectrum of metal sulphides but may be used as an initial basis to understanding the effects of dissolved ions on the electrical double layer. As such, any deviations from this theory should not be unexpected. A schematic diagram of the variation of zeta potential with an increase in ionic strength is shown in Figure 3.5:

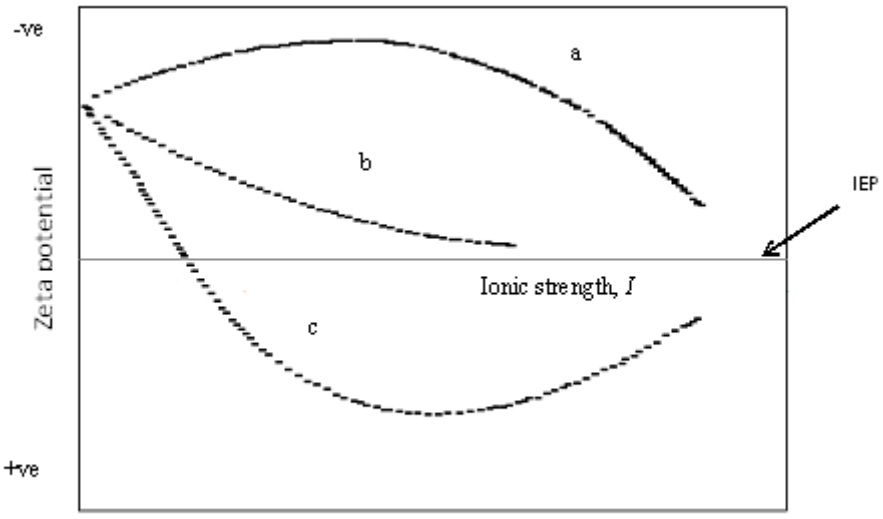

Figure 3.5: Variation of zeta potential with ionic strength (Söhnel & Garside, 1992)

Various attempts to modify surface charge by cation addition have been employed by several authors. Vergouw and co-workers (1998) suspended pyrite and galena particles, separately, into a 60 ppm suspension of Ca^{2+} ions. The addition of the Ca^{2+} ions had a significant effect on the charge properties of both the galena and pyrite particles. In both systems the zeta potential of the particles became less negative with calcium ion addition. The reduction in zeta potential for galena led to improved settling while in the case of pyrite, settling was actually retarded. This is somewhat consistent with the results presented by Mokone and co-workers (2012) and DiFeo and co-workers (2001). When Ca^{2+} ions were added to both CuS and ZnS systems Mokone and co-workers (2012) observed that the zeta potential of both particles became less negative. The study was however not extended to settling properties because the particles were assumed to fully obey the DLVO theory, implying an assumption that a decrease in zeta potential translated to an increase in agglomeration and settling. On the other hand, DiFeo and co-workers (2001) observed that the presence of Ca^{2+} ions on ZnS only led to a reduction in the magnitude of the zeta potential at low pH while no strong correlation was noted between settling velocities and zeta potential at high pH values.

A sphalerite suspension exhibited improved settling properties in the presence of Pb^{2+} ions while in the presence of Fe^{2+} ions settling of the particles was inhibited (Vergouw et al., 1998). This shows that different bivalent ions have varied effects on the zeta potential of different metal sulphide systems and hence are not equally successful as settling inducing additives.

Traditional flocculants such as Al^{3+} have also been used in metal sulphide systems to promote settling and, according to Mokone and co-workers (2012), Al^{3+} ions significantly reduced the magnitude of the zeta potential of CuS and ZnS particles by a factor up to almost 3. Undoubtedly the addition of bi- and trivalent ions and, in certain cases, other additives such as polymers can be used to promote settling in metal sulphide systems. Several challenges, however, arise from the use of additives and these may include: the additional cost associated with additives, how to de-activate them, removal of the more toxic variants such as Pb^{2+}ions and neutralising the chemical effects associated with certain additives such as the reducing/oxidising effects that maybe created by addition of certain ions. It would therefore

be preferable to reduce or prevent the use of additives in inducing settling hence the need to explore further surface modifying techniques.

3.2.3 pH control

By exploiting the zeta potential-pH behaviour of metal sulphide particles, Mokone and co-workers (2012) suspended CuS and ZnS particles, post precipitation, in varying solutions of modified pH, with values ranging from pH 3 to pH 11 with the expectation of observing the least magnitude in zeta potential at low pH values. For the ZnS system, the zeta potential fell within the non-repulsive range of -15 mV to +15 mV (Ottewill, 1982) at pH 6 and lower. In the case of CuS, the general trend observed was the same as that observed in the ZnS system, although the lowest magnitude of zeta potential achieved was about 25 mV at a pH of 3, not low enough to promote agglomeration.

Table 3.1: Dissolution pH of various metal sulphides

Metal Sulphide	Dissolution pH
Copper sulphide	0
Iron sulphide	< 5
Zinc sulphide	< 1
Nickel sulphide	< 3
Manganese sulphide	< 7

The method of pH control to induce settling post-precipitation has not been widely used in industry because of various major challenges. Table 3.1 shows the pH ranges at which selected suspended metal sulphide particles in solution begin to dissolve. As such, it should be noted that altering the pH of some metal sulphide suspensions in order to aid settling may actually be counterproductive as this would also reduce the solids concentration by promoting dissolution, which is detrimental to the cause of metal ion scavenging. Another challenge arises from the fact that most isoelectric values of metal sulphides are within low pH values and in order to improve settling the metal sulphide suspensions need to be rendered acidic. At

any pH values less than 6, the sulphide in solution, either residual from the precipitation process or as a result of metal sulphide dissolution, becomes stable as the $H_2S_{(aq)}$ species which has the potential of forming $H_2S_{(g)}$. Hydrogen sulphide gas poses a health and safety hazard to personnel and it may also be detrimental to the environment therefore whenever possible low pH should be avoided. Further to this challenge, treated wastewater has to be near neutral pH before it can be emitted into natural water reservoirs and as such acid water would need to be conditioned by pH modifiers such as NaOH at a further cost. Although technically feasible, in some cases, pH control post precipitation to induce settling is compromised by various operational challenges and as such cannot be seen as a solution to alleviate solid-liquid separation challenges in metal sulphide precipitation.

All the previously mentioned and reviewed techniques may, to some degree, be classified as conventional in as far as improving the particle size characteristics of metal sulphide precipitates. However, the fact that metal sulphide precipitation as a process is yet to be widely adopted in waste water treatment can be attributed to the inadequacy of the mentioned techniques in alleviating the solid-liquid separation challenges associated with sulphide precipitation. This challenge may be addressed two fold, improving existing techniques in order to optimise the respective processes or by researching on new mechanisms that may improve the viability of metal sulphide precipitation.

During sulphide mineral flotation the process of selective separation of minerals greatly depends on a number of factors that include effective control of the extent of surface oxidation on the mineral surface (Smart, et al., 1998). Oxidation together with the use of collector molecules is used to induce a hydrophobic surface during flotation. This promotes bubble attachment and consequently increases the zeta potential of highly negatively charged sulphide particles. Coincidentally, assuming that precipitated sulphide particles obey the DLVO theory, a less negative zeta potential is pre-requisite to inducing aggregation and subsequent particle sedimentation. The next section of this review will look at partial oxidation as a potential process to induce aggregation during metal sulphide precipitation by reducing the zeta potential magnitude of the particles and thus the subsequent inter-particle electrostatic repulsions.

3.3 Partial oxidation of metal sulphide particles

From the early electrophoresis-based studies on the surface chemistry of metal sulphides, an intrinsic pattern of low IEP values has been observed. Table 3.2 shows the IEP values reported from different studies on various metal sulphides. As will be discussed later, reducing conditions are necessary for the sulphides to exhibit this feature.

Table 3.2: IEP for metal sulphides

Sulphide	IEP	Reducing agent	Reference
FeS	3	N_2	Bebie et al., 1998
CoS	< 3		Liu and Huang 1992
Co_9S_8	3		Haruta et al., 1984
NiS	< 3	H_2	Goboeloes et al., 1984
NiS	2.5-3		Moignard et al., 1976
Cu_2S	< 5	N_2	Fullston et al., 1999
Cu_2S	< 3		Peng and Ourriban 2006
ZnS	4		Atkins and Pashley 1993
ZnS	3		Williams and Labib 1985
PbS	2.5	Ar	Fornasiero et al., 1994
PbS	< 2	N_2	Bebie et al., 1998
CuS	< 1	N_2	Liu and Huang 1992
CuS	< 2	N_2	Mokone et al., 2010

With the majority of metal sulphide IEP's within low pH values, as shown in Table 3.2, it follows that, for any pH values towards and beyond neutral pH, the zeta potential of the respective sulphide particles is highly negative. This, however, assumes no charge reversal, which may be possible in certain cases. Typical zeta-pH curves for ZnS, PbS and FeS are shown in Figure 3.6.

By analogy with metal hydroxides, several authors, including Kelebek and Smith (1989), state that the surface of transition metal sulfides is covered with >S-H groups. These surface functional groups are proton exchanging sites which render H^+ and OH^- potential determining ions. This notion is in unison within the observed trend in ζ-pH curves for transition metal sulphides, were the surface sites become protonated with a decrease in pH, resulting in the observed increase in zeta potential. The differences in the behaviour and rate of change of zeta potential with pH among the transition metal sulphides can then be attributed to the different surface acidity constants that arise from the different interactions between the S^{2-} and the respective Me^{2+} ions and structural differences between their exposed faces, by comparison with the oxides (Nortier, et al., 1997).

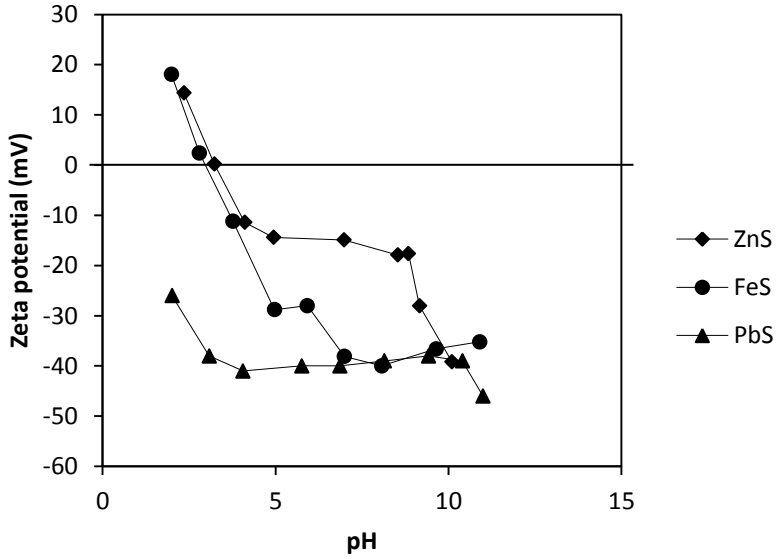

Figure 3.6: Typical ζ – pH behaviour for metal sulphides (Ref-Table 2.3)

With the introduction of oxygen to an aqueous metal sulphide system, surface modification can occur in 3 ways:

i. Mild oxidation to surface elemental sulphur

According to Moignard and co-workers (1977), the largely negative zeta potential of metal sulphides is due to the existence of surface elemental sulphur. The existence of this elemental

sulphur is attributed to the slight oxidation of the metal sulphide surface produced according to Equation 3.5.

$$MS + \frac{1}{2}O_2 + 2H^+ \rightarrow M^{2+} + S^0 + H_2O \qquad 3.5$$

This is supported by the fact that the IEP of elemental sulphur, as presented by Healy and Moignard (1976), is around a pH of 1.6. Clifford and Miller (1974) (as cited by Healy and Moignard (1976) also detected trace elemental sulphur on acid treated ZnS using x-ray photoelectron spectroscopy. The oxygen that is limiting in Equation 3.5 is considered residual from the process of purging dissolved oxygen that is inherent in most water systems. Butler and co-workers (1994) found that water purged with nitrogen can contain up to 0.5 ppm.

Moignard and co-workers (1977) also proposed that the surface oxidation of a metal sulphide can be accompanied by the simultaneous reduction of water as shown in Equation 3.6, thereby allowing the formation of elemental sulphur on the surface, even in the absence of dissolved oxygen.

$$MS + 2H_2O \rightarrow H_2 + S^0 + M(OH^-)_2 \qquad 3.6$$

$$MS + nH_2O + \frac{1}{2}n\ O_2 \rightarrow M_{1-n}S_{1-x} + xS^0 + nM(OH^-)_2 \qquad 3.7$$

Equation 3.5 and Equation 3.6 can be combined to form a general equation shown as Equation 3.7 (Fullston et al., 1999, Fornasiero et al., 1992 and Smart et al., 1998). The electrokinetic behaviour of the metal sulphides then depends on the ratio of the products in Equation 1.3, the extent of the reaction, the chemical form of the metal deficient surface and the particle interactions which include the level and extent of surface coverage by S^0 and or the oxygen compound species.

ii. Substitution of >S-H by >O-H

Bebie and co-workers (1998) stated that a metal sulphide in aqueous solution was expected to have at least two types of surface functional groups that include, the –Me-OH and –S-H groups. Moignard and co-workers (1977) show that, upon ageing, the IEP of ZnS shifts from low pH to up to about 8, the pH of the oxide. They attribute this shift to a modification of the surface with sulphur species gradually replaced by oxygenated species. Contrary to many statements in the literature, the replacement of the >SH group by the >OH group, according to Equation 3.7, is not an oxidation process in itself. Nevertheless, it is made possible by an oxidation process which results in the depletion of the S^{2-} species as it is oxidised in to the S^{6+} species as defined by Equation 3.9, thereby shifting the equilibrium in Equation 3.8 to the right.

$$>S\text{-}H + OH^- \leftrightarrow >O\text{-}H + SH^- \qquad 3.8$$

$$SH^- + 2O_2 \leftrightarrow SO_4^{2-} + H^+ \qquad 3.9$$

The effect of the oxidizing potential of the medium on the nature of the surface (sulfided or hydroxylated) is exemplified by the results of the work carried out by Bebie and co-workers (1998) on mineral and synthetic pyrite. After sparging nitrogen in water to purge dissolved oxygen, a 0.25 mmol/L solution Na_2SO_3 was added to the water to scavenge all the remaining oxygen through the formation of Na_2SO_4. The zeta potential of this un-oxidised pyrite was highly negative with an IEP of around 2. In such a case the negative charge cannot be attributed to the effect of surface elemental sulphur, but only to the acidity of >S-H groups.

Similarly, sparging an aqueous system with argon is also known to reduce the amount of dissolved oxygen to extremely low concentrations, compared to the concentrations that can be achieved by the use of nitrogen. In a study conducted by Fullston and co-workers (1999), the zeta potential of pyrite particles conditioned under a nitrogen atmosphere were compared to those conditioned under argon. The particles under nitrogen, as shown in Figure 3.7, had a slightly higher zeta potential than those conditioned under argon over the greater part of the

pH range. Fullston and co-workers (1999) termed the pyrite surface produced under argon conditioning as being closest to resembling that of 'virgin' pyrite and that produced under nitrogen as being affected by residual oxygen.

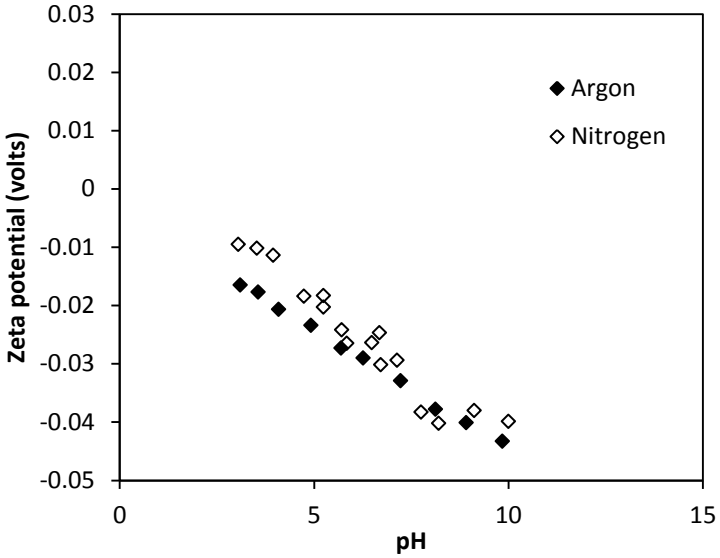

Figure 3.7: Zeta potential-pH curves after Nitrogen and Argon conditioning (Fullston, et al., 1999)

The results shown in Figure 3.7 seem to buttress two important concepts: the more negative surface charge of the metal sulphide particles under argon is largely due to the acidity of the >S-H group and the increase in the particle zeta potential under nitrogen is due to residual oxygen causing the substitution of the >S-H group by the less negative >O-H group. It should however be noted that the more negative charge exhibited by the metal sulphide particles under the argon environment may not only be due to the acidity of the >S-H group but also due to the formation of an elemental sulphur layer coupled with the reduction of water. This means that with oxygen addition into an aqueous metal sulphide system both mechanisms described in (i) and (ii) can simultaneously take place. The net effect on particle charge becomes dependent on the extent and dominance of either mechanism.

Fullston and co-workers (1999) found that the zeta potential of copper minerals exposed to oxygen for 60 min became less negative and even positive for copper mineral variations. The

effects of oxygen on the zeta potential of the minerals followed an oxidation series presented as chalcocite > tennantite > enargite > bornite > covellite > chalcopyrite (Fullston et al., 1999). This shows a variation on the effects of oxygen on different metal sulphide species. To this effect, the degree of oxidation should not be measured by the extent of oxygen exposure but in fact the position of the isoelectric point, in relation to that of the intrinsic metal sulphide, elemental sulphur and the respective metal hydroxide species. The isoelectric points of the respective metal sulphide species are shown in Table 3.3:

Table 3.3: IEP values of transition metals oxygen compounds

Element$^{(oxidation\ degree)}$	Oxygen compound	IEP Oxygen compound	Sulphur compound	IEP S^0
Fe^{2+}	$Fe(OH)_2$	12	FeS_2	
Co^{2+}	$Co(OH)_2$	11.4	CoS	
Ni^{2+}	NiO	10.3	NiS	
Ni^{2+}	$Ni(OH)_2$	11-12	NiS	
Cu^{1+}	Cu_2O	8.1	Cu_2S	1.6
Zn^{2+}	ZnO	8.7-10.3	ZnS	
Pb^{2+}	$Pb(OH)_2$	10-11	PbS	
Cd^{2+}	$Cd(OH)_2$	> 10.5	CdS	
Mn^{2+}	Mn(OH)2	7	MnS	

Although it has been established that sulphide minerals begin to oxidise with exposure to moisture and oxygen, Fornasiero and co-workers (1992) found that iron sulphide exposure to oxygen was ineffective and led to little or no change on the surface electrical properties of particles conditioned under neutral or basic conditions. As shown in Figure 3.8, particles conditioned at pHs 7 and 9 retained a similar ζ-pH behaviour to that of the 'virgin' metal sulphide after oxygen exposure. While the particles conditioned at pHs 5 and 6 underwent a shift in the IEP after oxygen exposure, the magnitude of the shift increased with a decrease in pH. The ζ-pH curve of 'virgin' iron sulphide is shown previously in Figure 3.6.

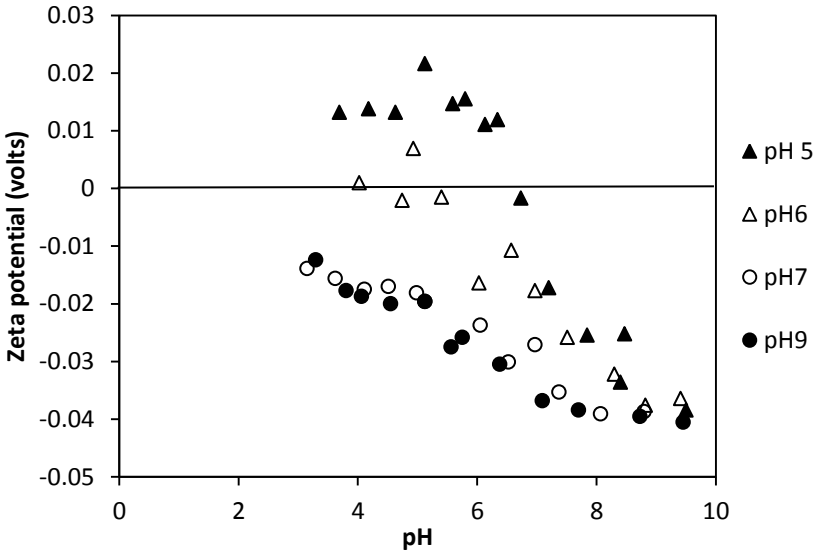

Figure 3.8: Oxidation effects after different pH conditioning of FeS (Fornasiero, et al., 1992)

This phenomenon, however, may vary from one metal sulphide system to another as Moignard and co-workers (1977) observed that the IEP for ZnS exposed to atmospheric oxygen shifts systematically to high values with increasing pH. This is the opposite trend to that observed by Fornasiero and co-workers (1992) on FeS. Duran and co-workers (1995) also observed a similar trend in studies on ZnS. From these electrokinetic measurements, a conclusion can be drawn that metal sulphide oxidation may have at least two independent variables, pH and dissolved oxygen.

3.4 Charge reversal by adsorption of hydrolysed ions

The ζ-pH pattern of transition metal sulphides can be made more complex by specific adsorption of hydrolysed cations. If any of the processes described in (i) and (ii) liberate any metal ions by dissolution, these ions may be specifically adsorbed onto the metal sulphide particle surface. Nicolau and Menard (1991) observed multiple isoelectric points for both ZnS and CdS in the presence of dissolved Zn^{2+} and Cd^{2+} ions respectively. Both zinc and cadmium metal sulphide systems had similar ζ-pH behaviour in the presence of hydrolysed metal ions and from that background, only the ZnS system will be reviewed. Figure 3.9 shows the zeta potential variation of zinc sulphide particles with pH after being suspended in

zinc sulphate and zinc chloride electrolytes respectively as observed by Nicolau and Menard (1991). The characteristic 'S shape' exhibited by the two curves was attributed to the activity of different potential determining ions (PDI) in solution as a result of the change in pH.

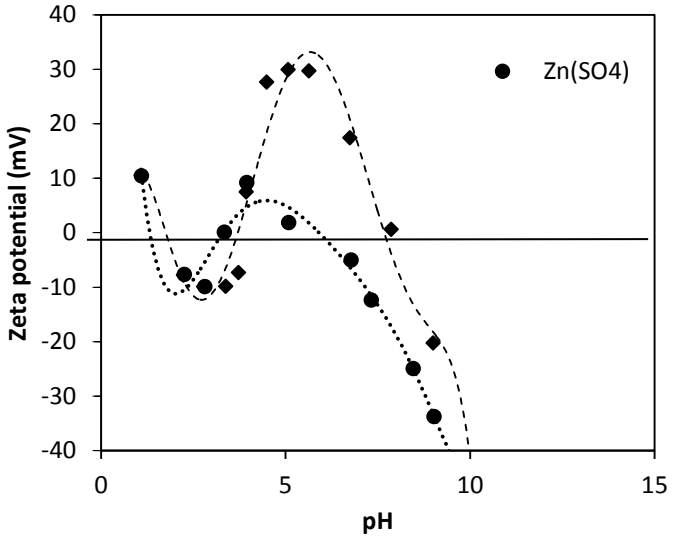

Figure 3.9: ζ-pH curves for ZnS particles in either 10^{-3}M solution of $ZnSO_4$ or ZnCl (Nicolau and Menard, 1991)

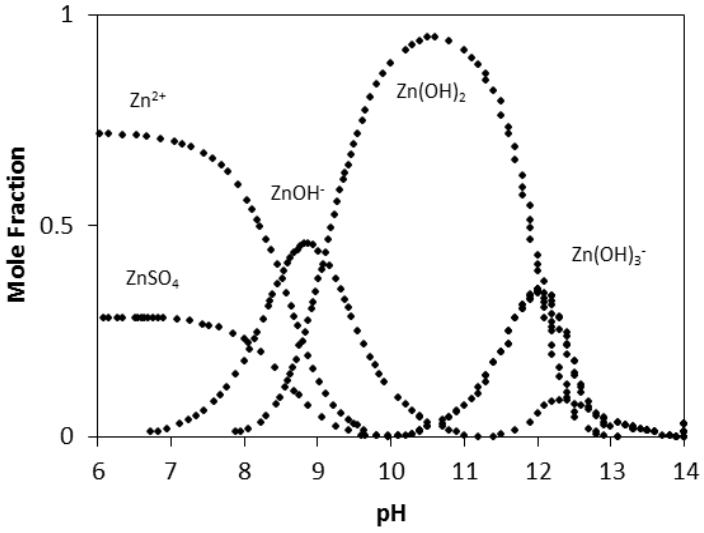

Figure 3.10: Concentration vs pH diagram showing different species in a $ZnSO_4$ solution (Nicolau and Menard, 1991)

Nicolau and Menard (1991) computed a concentration versus pH diagram for all the possible species found in a $ZnSO_4$ solution at different pH conditions. They found that the dominant species in solution under acidic conditions were the Zn^{2+} ions and to a lesser extent molecular $ZnSO_4$. As pH increased the dominant species changed from being the metal ion to the hydrolysed metal oxy/hydroxide species as shown in Figure 3.10. The zeta potential of the metal sulphide particles could then be considered to be a function of the interaction between the particle surface and the hydrolysed electrolyte species in solution and their respective potential determining characteristics.

Another feature of the graphs presented in Figure 3.9 as presented by Nicolau and Menard (1991) is the difference in the maxima between the two electrolyte systems. This was attributed to the identity of the anion and was said to follow the following series max ζ_{Cl^-} > max $\zeta_{SO_4^{2-}}$. In the case of a single electrolyte, the maximum was found to depend on the concentration of the anion.

As mentioned earlier, introducing oxygen to an aqueous system of metal sulphide particles results in a number of complex processes that alter the surface properties of the metal sulphide particles. These individual processes may interact synergistically or antagonistically on the resultant particle surface charge.

3.5 Characterisation methods

Fullston and co-workers (1999) reported that the zeta potential of sulphides is very sensitive to surface oxidation with a change in magnitude of up to 80 mV including a sign reversal, between a non-oxidised and fully oxidised surface. Taking into account such sensitivity, it would be ideal to characterise the surface of metal sulphides using an in-situ analytical technique. This ensures that the particle surface is analysed without any disturbance or contamination as a result of sampling or pre-treatment. Smart and co-workers (1998) used a number of surface sensitive ex-situ measurement techniques that include SEM (Scanning Electron Microscopy), XPS (X-ray Photoelectron Spectroscopy) and SAM (Scanning Auger Microscopy). The advantages of using such techniques would include obtaining the

compositional analysis of the surface, spatial distribution of adsorbed species and the chemical states of surface atoms. Although this information may be invaluable in monitoring surface changes due to oxidation, it is of equal importance to couple it with a validation of the relationship between the measured surface properties with the prevailing surface properties of particles in the oxidation reactor before sampling.

In some cases however, it may be adequate to measure the net effect of the surface species interactions on the surface charge and potential. Electrophoresis may be adequate for this. The characterisation of various metal sulphides using this technique has, however, led to the reporting of a wide range of zeta potential values and iso-electric points for the respective metal sulphides. **Error! Reference source not found.** shows a variation in measured IEP values from different zinc sulphide studies. The differences in these reported values can be attributed to poor control of experimental conditions and, to a lesser extent, the slight variations in the chemical nature of the metal sulphide particles. Consequently, if electrophoresis is to be used as an analytical technique, any precipitated metal sulphide particles should be characterised within their context of production and storage. The reported literature values can however be used as reference values.

Table 3.4: Measured IEP values for ZnS

Metal Sulphide	IEP	Reference
ZnS	2.3	Nicolau and Menard, 1991
ZnS	4	Vergouw et al., 1998
ZnS	2.5-6	Duran et al., 1995
ZnS	4	Moignard et al., 1977
ZnS	3	Williams and Labib, 1985
ZnS	3-3.8	Mokone et al., 2010

3.6 Surface complexation model: CD-MUSIC

The charge distribution (CD) multi-site-complexation (MUSIC) model was originally formulated as a speciation model for predicting the development of surface charge of metal oxide/hydroxide species (Hiemstra, et al., 1989). In the current work, the CD-Music model will be modified in an attempt to simulate the surface of copper sulphide particles produced experimentally. Firstly the basis of CD-Music will be described in relation to metal oxide/hydroxide surfaces, attributing to similarities or deviations with metal sulphide surfaces. When a metal oxide/hydroxide particle is immersed in an aqueous suspension the particle develops charge, among other factors, due to the existence of different types of groups on the particle surface. Hiemstra and co-workers (1989) acknowledged that these surface groups may be attached to single, double or triple coordinated atoms in the crystal lattice. The reactivity of the surface group would then depend on the coordination of the lattice atom to which the surface group is attached. Kelebek and Smith (1989) and Nicolau and Menard (1991) propose the existence of two surface functional groups on the surface of metal sulphides, the hydroxyl group (>Me-OH) and the thiol group (>S-H). Therefore, the charge of a metal sulphide surface will be governed by the nature and number of the mentioned groups.

In the absence of direct measurement techniques it is very difficult to assign charge to the different surface groups that can exist on a surface. In dealing with metal oxides/hydroxides Hiemstra and co-workers (1989) used the electrostatic valence to determine the partial charge of a surface group. Electrostatic valence in a crystal was introduced by Pauling (1962) and is defined as shown in Equation 3.10:

$$\nu = \frac{z_{cation}}{CN_{cation}} \qquad 3.10$$

Were ν is the valence or "strength of the electrostatic bond", z_{cation} is the formal charge and CN_{cation} is the coordination number of the cation respectively. Pauling (1962) went on to postulate that the charge of an anion within the same crystal is equally neutralised by all the cations to which it is attached to and this leads to the formulation of Equation 3.11:

$$\nu = \frac{z_{cation}}{CN_{cation}} = \frac{z_{anion}}{CN_{anion}} \quad 3.11$$

Consequently according to the model developed by Hiemstra and co-workers (1989) a coordinately unsaturated cation, as it exists on the surface of an oxide will impart a charge ν to an adsorbed hydroxyl group, with the resultant partial charge being ν-1. In the case of sulphides and specifically a thiol group, an adsorbed HS^- ion will have a resultant partial charge of ν-1 upon attachment to a lattice cation.

The acidity of the adsorbed thiol group depends on the structural properties of the crystal lattice. With respect to hydroxides it may be said that the acidity of the hydroxyl group depends on the extent of the electron withdrawing effect of its environment. For all the hydroxyl groups attached to a surface, it follows that the most acidic will be the one which undergoes the largest electron withdrawing effect from its environment. Hiemstra and co-workers (1989), also proposed that the higher the electrostatic potential created by the nearest cations at the surface, the more acidic the group. Hence, the first order effect is the coordinence of the hydroxyl group with an order of increasing acidity: $-OH(_{1c}) < -OH(_{2c}) < -OH(_{3c})$ and so on, were c is coordination, and the second order effect will be the coordinence of cations (Nortier, et al., 1997). In the case of sulphides, the change in pH up to neutral pH is due to the protonation or de-protonation of the thiol group. The affinity of the H^+ ions to the surface thiol group can thus be assumed to depend on the respective acidity constants which in turn depend on the coordination of the thiol group on the copper sulphide surface.

3.7 Hypotheses

It was the aim of this project to improve the solid-liquid separation characteristics of transition metal sulphide particles from solution by the promotion of effective aggregation

and subsequent settling, post-precipitation. This was achieved by testing two hypotheses that were bound by the following operating conditions:

i. The pH of all post precipitation processes was set at a pH of 6 to prevent excessive dissolution of metal sulphide oxidation products and to limit the addition of pH modifying agents subsequent to the metal sulphide precipitation process at a pH of 6.
ii. After post-precipitation treatment and subsequent settling analysis, the total dissolved metal ion concentration was not to exceed 5% of the synthetic waste water metal ion concentration. Any concentration above this value rendered the treatment technique unsustainable as it reduced its viability. The metal ion concentration of 5 % was chosen solely on an investigative basis as an acceptable limit for dissolved ions in solution.

The hypotheses tested are:

i. Suspending metal sulphide particles in a metal ion electrolyte will improve settling by reducing the effective zeta potential of the metal sulphide particles and improve aggregation.
ii. Controlled partial oxidation of metal sulphide particles promotes settling by inducing surface modifying effects that reduce the magnitude of the zeta potential and thus cause an increase in aggregation.

4 Materials and Methods

4.1 Experimental design

The investigation was divided into two phases. The first part focused on the precipitation of metal sulphide particles and the effect of metal and sulphide ions on the zeta potential and subsequent settling characteristics of the particles, post precipitation. In the second part of the study, the effect of partially oxidising the precipitated particles was investigated in relation to metal ion dissolution and settling properties.

4.2 Metal sulphide precipitation

4.2.1 Reagents

All chemicals used in the experiments were of analytical grade obtained from Merck and Sigma-Aldrich. The reagents used include $CuSO_4.5H_2O$, $Na_2S.9H_2O$, KCl, NaOH and HCl. Nitrogen used was obtained from Afrox South Africa.

4.2.2 Experimental set-up

All the precipitation experiments were carried out at 25 °C, atmospheric pressure and in a 1 L continuously stirred tank glass reactor with a working volume of 0.9 L and equipped with four baffles. A schematic representation of the set-up is shown in Figure 4.1. The reaction vessel was covered at the top with a lid that had 7 ports for the sulphide resistant pH probe, REDOX probe, overhead stirrer, reagent feed, nitrogen sparger and an acid/base dosing port. Agitation within the reaction vessel was achieved via an impeller connected to an overhead variable speed motor. The reagents were pumped into the reactor using calibrated Watson Marlow 520S (Falmouth, UK) pumps.

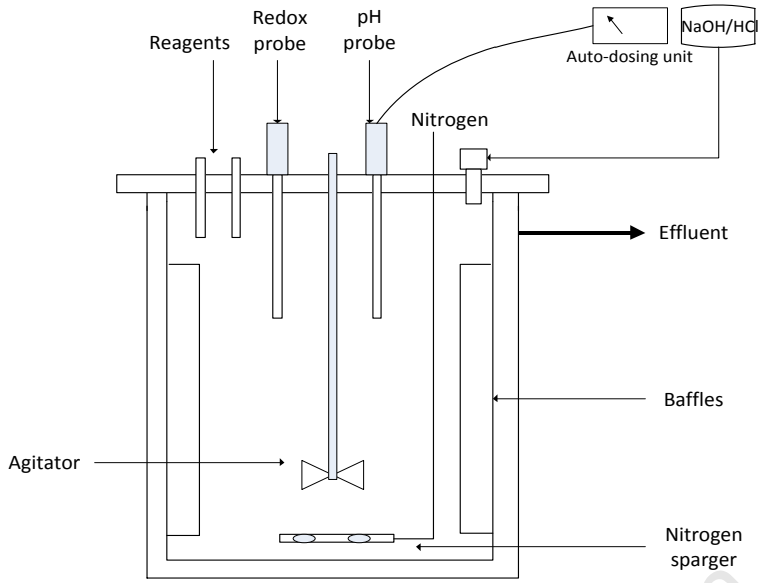

Figure 4.1: Schematic view of the CSTR set-up for the precipitation of CuS

An automatic dosing unit, Metrohm 800 Dosino Unit (Switzerland), was used to control the pH of the reaction vessel at the desired value by adding either 0.5M HCl/0.5 M NaOH as required. The dosing unit was connected to a sulphide resistant pH probe from Metrohm AG (Switzerland) which was calibrated using Merck buffer solutions at pH 4.01 and 7 before the start of each experiment. Redox was measured using a Pt and Ag/KCl probe supplied by Metrohm AG (Switzerland). The nitrogen sparged in the reaction vessel was 99.999 % pure and with a 0.35 ppm oxygen content.

4.3 Precipitant partial oxidation

4.3.1 Reagents

Medical oxygen at a purity level of > 99.5%, was used for the oxidation experiments. It was regulated from a pressurised cylinder to 1 bar and then flow controlled using a rotameter.

4.3.2 Experimental set-up

The oxidation reactions were conducted in a 1 L batch reactor fitted with four baffles and fitted with a sparger. Agitation was achieved via a four pitched blade impeller connected to an overhead variable speed motor. A Microprocessor pH Meter (pH 212) from Hanna Instruments was used to measure the pH. The meter was calibrated using Merck buffer solutions at pH 4.01 and 7 before the start of each experiment. Redox inside the reactor was measured using a Pt and Ag/KCl probe from Metrohm AG (Switzerland).

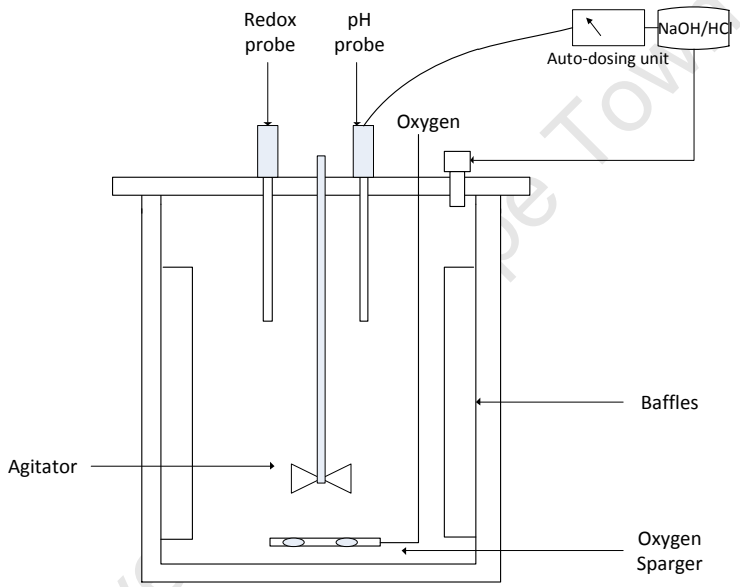

Figure 4.2: Oxygen bubbling reactor for the partial oxidation of CuS particulates

4.4 Analytical techniques

4.4.1 Zeta potential

A dynamic back light scattering technique (Malvern Zetasizer Nano ZS model) was used to measure the zeta potential of the particles. The zeta potential-pH curves were produced using the MPT-2 Autotitrator in conjunction with the Malvern Zetasizer Nano. The autotitrator was

connected to a sulphide resistant pH probe which was inserted into the sample measurement cell. Sample pH adjustment was achieved by the addition of either 0.2 molar HCl or 0.2 molar NaOH.

4.4.2 Settleability

A solids settleability test was performed using an Imhoff cone mounted on a cone stand. The method involved adding a litre of a well-mixed test suspension into the Imhoff cone and then leaving it to stand for 45 minutes. Before allowing the suspension to stand for a further 15 minutes, a rod was gently run on the inside of the cone to loosen any solids clinging to the sides. The results were measured in millilitres of settled solids per litre of solution. If any liquid pockets were observed between the settled particles the liquid volume was estimated and then removed from the volume of settled solids. The test was performed at room temperature and the top of the Imhoff cone was covered during settling to limit possible oxidation from atmospheric oxygen. It is critical to state that, the larger the volume of settled solids, the better the settling properties of the respective particles.

4.4.3 Dissolved metal ion concentration

Inductively coupled plasma optical emission spectrometry analysis (ICP-OES) was used to determine the dissolved metal ion concentration. All solutions were filtered through a filter paper with a pore size of 0.20 µm before analysis.

4.4.4 Chemical and micro-structural analysis

XRD was used for all chemical and micro-structural analysis of metal sulphide precipitant material.

4.4.5 Surface complexation model

A Microsoft Component Object Model (COM), which allowed IPhreeqc to be used by Matlab® through a COM server, was used to perform CD-Music calculations. By embedding IPhreeqc into Matlab®, the model was fitted to the experimental data using Matlab's routine lsqcurvefit. In order to produce the 'best' model fit to the experimentally obtained ζ-pH values, the following variables were optimised: density of surface species, respective acidity constants and adsorption of solution species to the surface. The optimised parameters were then assumed to be dominant on the surface of the respective CuS particles.

4.5 Experimental procedures

4.5.1 Metal sulphide precipitation

The experiments were conducted at room temperature (≈20°C) and pressure. All solutions were made up to the desired concentrations using de-oxygenated and Millipore de-ionised water. Water de-oxygenation was achieved prior to solution preparation by boiling the de-ionised water for at least 10 minutes then allowing it cool in a closed container. During solution preparation, oxygen contamination was avoided by sparging nitrogen whenever the vessel containing the solution was open to the atmosphere. Metal ion solutions were made up to a concentration of 500 mg/L and the sulphide ion solution concentration was made equi-molar to the metal ion concentration. Both stock solutions were stored in 10 litre graduated vessels equipped with two ports, one for solution withdrawal and the other for nitrogen sparging.

A CSTR was filled to the mark with de-ionised water after which the overhead stirrer was switched on and set at 650 rpm. Nitrogen gas was sparged through the reactor for 30 minutes before the reagents were pumped into the reactor simultaneously via the peristaltic pumps. The reagent flowrate was kept constant at 0.5 L min^{-1} throughout the experiment for both the reagents. Fluctuations in reagent flowrate were monitored using the graduations on the stock solution vessels in the event of any deviations in peristaltic pump performance. In the event of a flowrate variation between the metal ion stream and sulphide ion stream, the experiment

was aborted. Oxygen contamination in the stock solution vessels was prevented by continuous nitrogen sparging. The pH was controlled at pH 6 throughout the entire experiment by either the addition of 0.5 M HCl or 0.5 M NaOH and REDOX was recorded after every 2 minutes.

The sulphide concentration was measured after every 5 min to ascertain achievement of steady state. After the attainment of steady state, which took about 30 min, a sample for XRD and zeta potential analysis was collected after every 10 minutes for a further 150 minutes. Oxygen contamination of the collected metal sulphide suspension was avoided by sparging nitrogen in the collection vessel.

4.5.2 Effect of metal and sulphide ions on settling

Table 4.1: Experimental labelling

Concentration of ions (S-Sulphide, M-Copper)	Batch 1	Batch 2	Batch 3
(S) 7 mg L^{-1}	S2(a)	S2(b)	S2(c)
(S) 12 mg L^{-1}	S1(a)	S1(b)	S1(c)
0	E(a)	E(b)	E(c)
(M) 15 mg L^{-1}	M1(a)	M1(b)	M1(c)
(M) 25 mg L^{-1}	M2(a)	M2(b)	M2(c)

After completion of the precipitation step, five 1 L containers equipped with lids and labelled as per column, Batch 1, in Table 4.1 were filled with 0.95 L of the metal sulphide suspension and 0.05 L of the conditioning solution. The conditioning solution contained an appropriate concentration of KCl as an indifferent electrolyte and either metal or sulphide ions as the solution chemistry modifying agent. After conditioning, solution E did not contain any added metal or sulphide ions, solution M1 and M2 contained 15 mg L^{-1} and 25 mg L^{-1} of added metal ions respectively and solutions S1 and S2 contained 7 mg L^{-1} and 12 mg L^{-1} of the

added sulphide ions respectively. The amount of added metal ions in solutions M1 and M2 represented 3 % and 5 % of the metal ion stock solution respectively while that of added sulphide ions in solutions S1 and S2 represented 3 % and 5 % of the sulphide ion stock solution respectively.

All the vessels were gently agitated for 15 min under nitrogen before a sample was collected from each of the 5 suspensions for zeta potential analysis. The remaining part of the solution was measured for settleability. This experimental procedure was repeated three times to ensure reproducibility.

4.5.3 Partial oxidation of metal sulphide particles

The precipitation step of this experiment is as described in section 3.5.1. Once the metal sulphide particles were produced, samples were taken for zeta potential, XRD, metal ion concentration and settleability analysis. For the oxidation experiment, a litre of the metal sulphide suspension was placed in an oxygen sparged batch reactor and agitated at 350 rpm to avoid particle breakage. Oxygen was supplied into the reactor via a single ring sparger at a rate of 5 L min^{-1}. The REDOX potential was recorded after every 2 minutes and pH was kept constant at a pH of 6 by the addition of either HCl or NaOH. The experiment was run for 30 minutes before samples were withdrawn for zeta potential, metal ion concentration and XRD analysis while the metal sulphide suspension remaining in the reactor was emptied into an Imhoff cone for settleability analysis. The procedure was repeated for different residence times of the metal sulphide particles in the batch reactor. Oxygen was bubbled into the reactor for 60 minutes, at the same flowrate (5 L m^{-1}), before samples for XRD, zeta potential and metal ion concentration analysis were withdrawn from the reactor. The metal sulphide suspension in the reactor was emptied into an Imhoff cone for a settleability analysis. All the experiments were performed in triplicate in order to determine the accuracy of the experiments. The zeta potential measurements were performed within 5 minutes of experiment completion while settleability measurements commenced immediately after oxygen bubbling was stopped.

5 Results and discussion

5.1 Effect of metal and sulphide ions on settling

In this section, the effect of metal ions and sulphide ions on the zeta potential and subsequent settling properties of CuS is presented and discussed. The main aim of the investigation was to reduce the zeta potential magnitude of the metal sulphide particles, by making the charge less negative, in order to increase particulate sedimentation at a specific operating pH. The main emphasis was on investigating the relationship between the solution chemistry, in respect to lattice ion concentration, with the particle zeta potential and the particle settling characteristics. The ζ – pH behaviour of the metal sulphide particles beyond the operating pH was not considered. The results presented in Figure 5.1 show the effect of metal ion concentration on the zeta potential of CuS particles and the resultant settling characteristics.

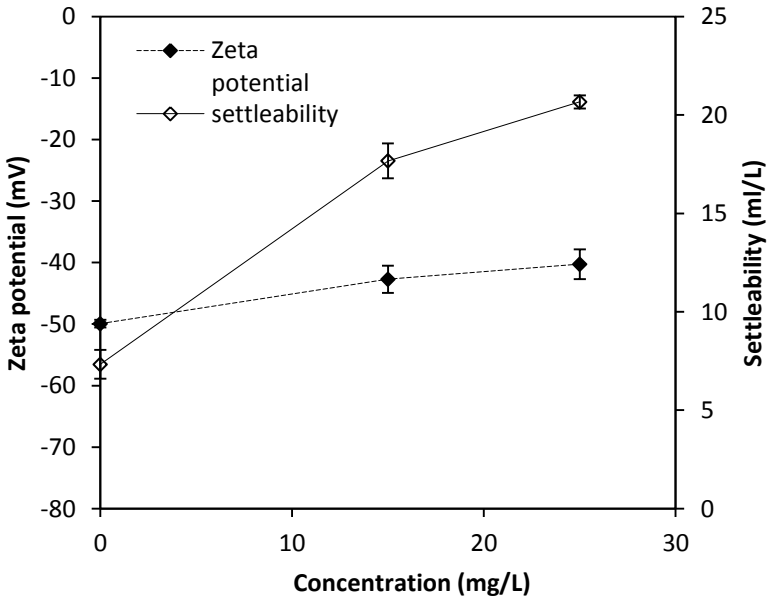

Figure 5.1: Zeta potential and settleability of CuS as a function of Cu^{2+} ion concentration.

Immediately after precipitation the CuS particles had a zeta potential of about -50 mV and a settleability value of 7 mL/L. As the solution chemistry was modified by increasing the

concentration of Cu^{2+} ions, an increase in the respective CuS particle zeta potential and settleability was also observed. A suspension, with an intermediate Cu^{2+} ion concentration of 15 mg/L resulted in particles that had a zeta potential of -42.7 mV and a settleability of about 18 mL/L. The associated rate of change in zeta potential with relation to the Cu^{2+} ion concentration was about 0.46 mV for every milligram of copper ions. A maximum zeta potential of -40 mv was attained when the CuS particles were suspended in a solution with a concentration of 25 mg/L of Cu^{2+} ions and these had a maximum settleability of about 21 mL/L. The associated rate of change in zeta potential with relation to the Cu^{2+} ion concentration was 0.24 mV for every milligram of Cu^{2+} ions added, about half the respective rate observed for the intermediate Cu^{2+} ion concentration. The maximum settleability observed, at a concentration of 25 mg/L of Cu^{2+} ions, was nearly 3 times more than that of the CuS particles produced immediately after precipitation.

Figure 5.2 shows the effects of S^{2-} ion concentration on both zeta potential and settleability of CuS particles. The data points corresponding to 0 mg/L of S^{2-} ions in Figure 5.2 are the same data points corresponding to 0 mg/L of Cu^{2+} ions in Figure 5.1.

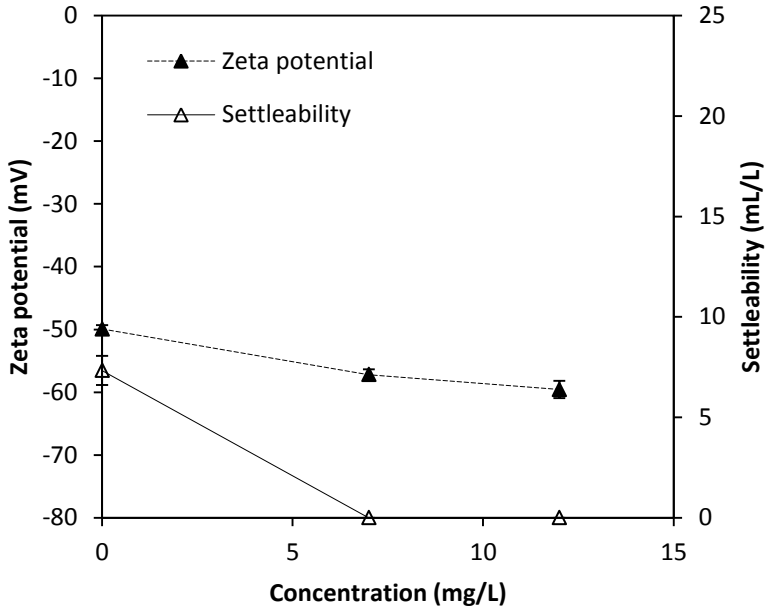

Figure 5.2: Zeta potential and settleability of CuS as a function of S^{2-} ion concentration.

As the concentration of sulphide ions was increased, the respective zeta potential of the CuS particles and the observed particle settleability decreased. The particles suspended in a solution with a S^{2-} ion concentration of 7 mg/L had a zeta potential of -57.2 mV. This translated to a decrease in zeta potential of about 7 mV and an associated particle settleability of 0 mL/L. A subsequent increase in the concentration of S^{2-} ions led to a further decrease in the zeta potential of the CuS particles and no change in settling characteristics.

5.1.1 Charge development

The charge on the surface of a divalent metal sulphide particle in an aqueous solution depends on, among other factors, the density and hydrolysis of the uncoordinated metal and sulphide atoms at the surface (Israelachvili, 1992). The effect of increasing the concentration of lattice ions on the zeta potential of some suspended metal sulphide particles is known but not very well understood (Lyklema, 1976). It is with this background and in an attempt to develop a balanced discussion that a number of mechanisms to explain the effect of lattice ions on zeta potential will be presented.

The results presented in Figure 5.1 and Figure 5.2 show a clearly defined trend in the zeta potential of the CuS particles after the addition of Cu^{2+} and S^{2-} ions. With the addition of Cu^{2+} ions, an increase in zeta potential is observed while a decrease in zeta potential is observed with the addition of S^{2-} ions. Since pH has been kept constant, it is reasonable to assume that the Cu^{2+} and S^{2-} ions are potential determining ions. This is also reinforced by the fact that the observed effect after ion addition increases with an increase in concentration of the respective ions and is also consistent with work carried out by Williams and Labib (1985), Fornasiero and co-workers (1992), Nicolau and Menard (1991) and Mokone and co-workers (2010). An indifferent electrolyte is used to maintain ionic strength and hence constriction of the electrical double layer will not be considered. After a review of various work on the effects of lattice ions on zeta potential of metal sulphide particles, Dekkers and Schoonen (1994) proposed that hydrolysis of uncoordinated surface atoms leads to two surface sites, a thiol group (>SH) and a metal hydroxide group (>MeOH), which is also consistent with the work carried out by Lyklema (1976). Evidently, from the results presented in Figure 5.1 and Figure 5.2, the zeta potential charge on the CuS particles is dependent on

the activity of the dissolved lattice ions including the ratio that exists between the two ion species in solution. Nicolau and Menard (1991) proposed chemisorption of metal ions on to S Bronsted sites according to Equation 5.1:

$$>S\text{-}H + Cu^{2+} \rightarrow >S\text{-}Cu^{+} + H^{+} \qquad 5.1$$

$$>Cu\text{-}OH^{+} + S^{2-} \rightarrow >Cu\text{-}S^{-} + OH^{-} \qquad 5.2$$

With an increase in Cu^{2+} ions, the forward reaction of Equation 5.1 is favoured and this results in an increase in the number of positively charged surface sites resulting in an increase in zeta potential as observed in Figure 5.1. Likewise, with the addition of S^{2-} ions the forward reaction as defined by Equation 5.2 becomes dominant. This depletes the number of positively charged species on the surface of the CuS particles and replaces them with negatively charged surface species resulting in a decrease in zeta potential. A decrease in zeta potential after sulphide addition is consistent with the presented results in Figure 5.2. Metal ions in solution are hydrolysed and according to Faur-Brasquet and co-workers (2002), the dominant copper species in solution at pH 6 and higher is the $Cu(OH)_n^{2-n}$ species. In this case the Cu^{2+} ions in Equation 5.1 may be replaced by the respective copper hydroxide species.

From the initial 0 mg/L suspension, the change in zeta potential was 0.48 mV for every milligram of Cu^{2+} ions added up to a suspension concentration of 15 mg/L. A further increase in Cu^{2+} ions from 15 mg/L to 25 mg/L resulted in a retarded zeta potential change of 0.24 mV for every milligram of Cu^{2+} ions added per litre of solution up to a concentration of 25 mg/L. The same trend is also observed in the case of S^{2-} ions, zeta potential changes at a rate of 1.04 mV for every milligram of S^{2-} ions added up to the intermediate sulphide concentration. The respective settleability drops significantly at the intermediate and maximum sulphide concentration to a zeta potential change of about 0.47 mV for every milligram of S^{2-} ions added per litre of solution. This may be consistent with the incremental saturation of Cu^{2+} and S^{2-} ions adsorbing sites on the surface.

Alternatively, a different mechanism can be proposed for the observed trends in Figure 5.1 and Figure 5.2. Everett (1988) stated that differential dissolution of ions from a surface may lead to the development of surface charge. If a CuS particle is immersed in de-ionised water, dissolution will occur until the ionic product is equivalent to the ionic product as shown in Equation 5.3:

$$[Cu^{2+}][S^{2-}] = K_{sp} = 8 \times 10^{-37} \quad 5.3$$

In the case that an equal amount of ions dissolve $[Cu^{2+}] = [S^{2-}] = 8.94 \times 10^{-19}$, a certain amount of copper based and sulphide based sites are present on the surface of the CuS particle. Their spatial orientation and surface density would depend on the crystal structure. If the concentration of any of the lattice ions in solution is increased, the respective dissolution of the ion from the crystal lattice should decrease according to the common ion effect. This mechanism however hinges on the applicability of the common ion effect at very low ion concentrations such as the case for metal sulphides. After the addition of Cu^{2+} ions into a suspension of CuS particles, there is a slight decrease in the dissolution of Cu^{2+} ions. This results in an increased density of positively charged species on the particle surface and the opposite can be assumed true in the case of S^{2-} ions.

5.1.2 Settling characteristics

No conventional and commonly agreed method exits for quantifying the extent of aggregation in a suspension. Mirnezami and co-workers (2003) summarised different ways of quantifying aggregation by the analysis of one or more of the following measurements: settling rate, viscosity, optical microscopy, particle size distribution, atomic force spectroscopy and turbidity. The settleability measurements presented in Figure 5.1 and Figure 5.2 can therefore be used as a measure of aggregation. According to the DLVO theory aggregation can be induced by decreasing the magnitude of inter-particle electrostatic forces and experimentally this entails reducing the zeta potential of particles. According to the zeta potential and settleability results presented in Figure 5.1 and Figure 5.2, an increase in the settleability of CuS particles is associated with a magnitude decrease in zeta potential while a

decrease in settleability is associated with an increase in zeta potential which is consistent with reducing and then increasing the inter-particle repulsive forces respectively. The interaction of electrostatic and van der Waals forces of the CuS particles have been calculated and are shown in Figures 5.3-5.5. They represent CuS particles immersed in an indifferent electrolyte, 15 mg/L Cu^{2+} ions and 7 mg/L S^{2-} ions.

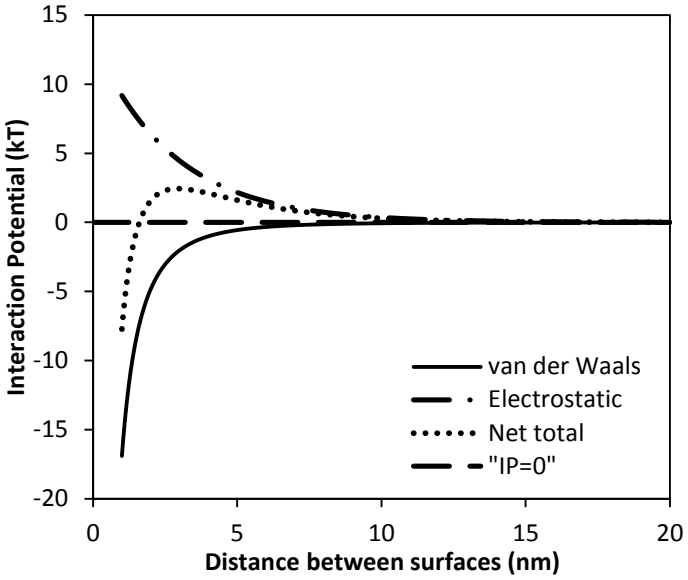

Figure 5.3: DLVO profile of CuS particles in an indifferent electrolyte

In calculating the DLVO profiles, using Equations 2.19 and 2.21 in the theory section, a Hamaker constant of 4×10^{-19} J was used (Horzempa & Helz, 1979) and the average particle radius was taken as 5 nm. By changing the zeta potential of CuS particles by lattice ion addition while maintaining a constant ionic strength, the main variable was the magnitude of electrostatic forces, which are repulsive in nature. As stated earlier, the stability of a suspension is based on the net interaction between the repulsive and attractive forces and this net interaction for CuS particles with no added lattice ions is shown in Figure 5.3 and labelled as 'Net total'. The observed settleability for this system is about 7 mL/L and this is governed by the rate of particle aggregation which in turn depends on the maximum energy barrier that exists between two colliding particles. According to the DLVO theory increasing the energy barrier would result in a decrease in the aggregation rate while the opposite is valid. The CuS particles suspended in an indifferent electrolyte without any added lattice ions will be used as

the reference point. A settleability rate of 7 mL/L corresponds with a zeta potential of about -50 mV and an associated maximum interaction potential of 2.44 kT.

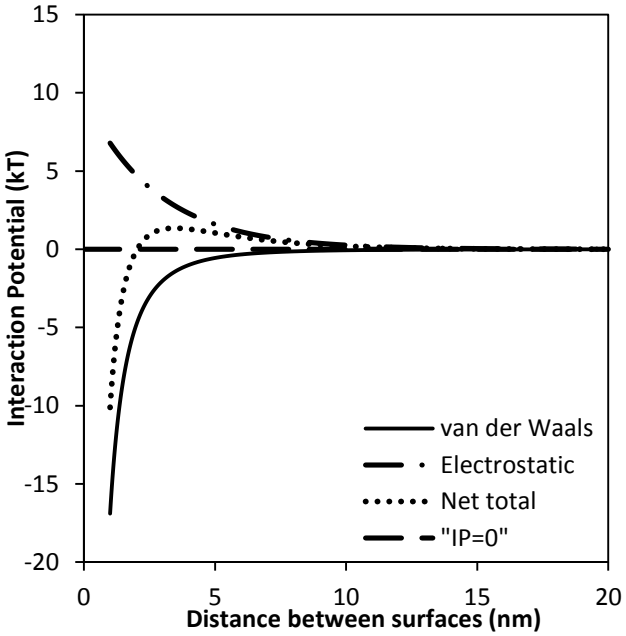

Figure 5.4: DLVO profile of CuS particles suspended in a solution of Cu^{2+} ions

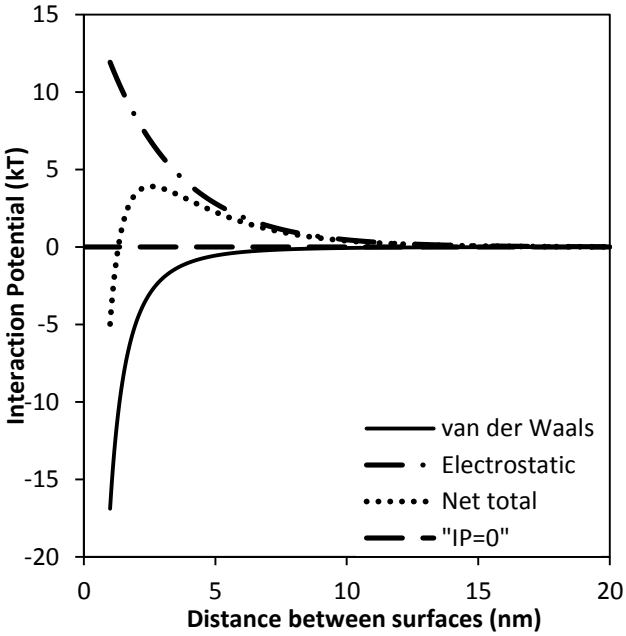

Figure 5.5: DLVO profile of CuS particles suspended in a solution S^{2-} ions

After the addition of Cu^{2+} ions the zeta potential of the CuS particles increases to – 43 mV. In comparison to the set reference point the maximum interaction energy reduces to 1.35 kT. According to the DLVO theory this should result in an increase in the rate of aggregation which is consistent with the observed increase in settleability from 7 mL/L to 17 mL/L. In the case of S^{2-} ion addition, the zeta potential of the CuS particles decreases to about -57 mV. This results in an increase in the electrostatic forces and hence inter-particle repulsion and in comparison with the set reference point the interaction potential increases to 3.91 kT, a value that should retard aggregation. This is consistent with the observed decrease in settleability from 7 mL/L to 0 mL/L.

5.2 Effect of partial oxidation on zeta potential

5.2.1 Operating conditions

The operating pH in the precipitation reactor was kept constant by the automated addition of either HCl or NaOH and this resulted in an effective reactor pH of 6 ± 0.1. Redox potential was monitored from the start of the experiment but was only recorded after steady state (Approx 30 min from the start of the experiment), with respect to sulphide ion concentration, had been attained. The results of redox potential recorded for the first 75 min of the precipitation reaction are shown in Figure 5.6:

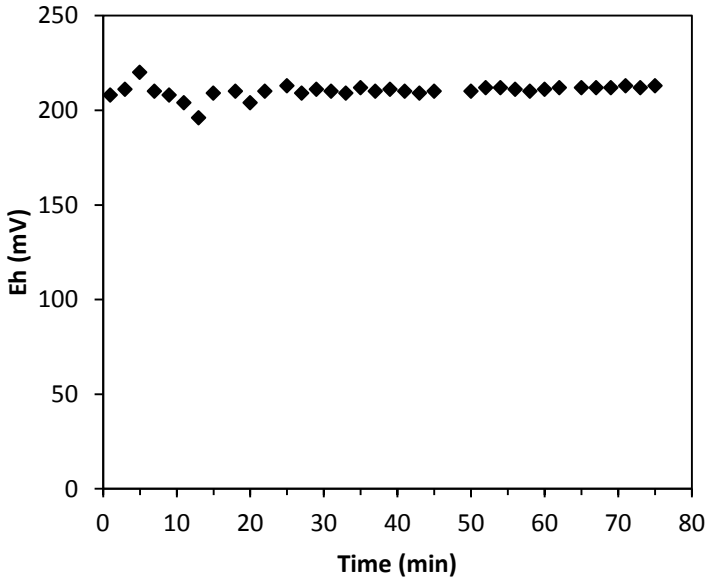

Figure 5.6: Measured redox potential during CuS precipitation

After steady state was attained, the redox potential fluctuated for the first 15 min before it remained relatively constant around a potential of 210 ± 3 mV. The observed fluctuations were due to the system stabilising after removal of the sulphide probe, removal of the probe reduced the partial pressure of nitrogen in the relatively closed reactor which affected the bulk redox conditions in the reactor. A plastic seal was used to close the sulphide probe port in order to maintain a slight nitrogen pressure head in the reactor. This was consistent for all three precipitation experiments. The most consistent residual oxygen concentration achieved was about 0.35 ppm.

A Pourbaix diagram maps the possible stable equilibrium phases of an aqueous electrolyte system and one such diagram for a Cu-S-O system is shown in Figure 5.7

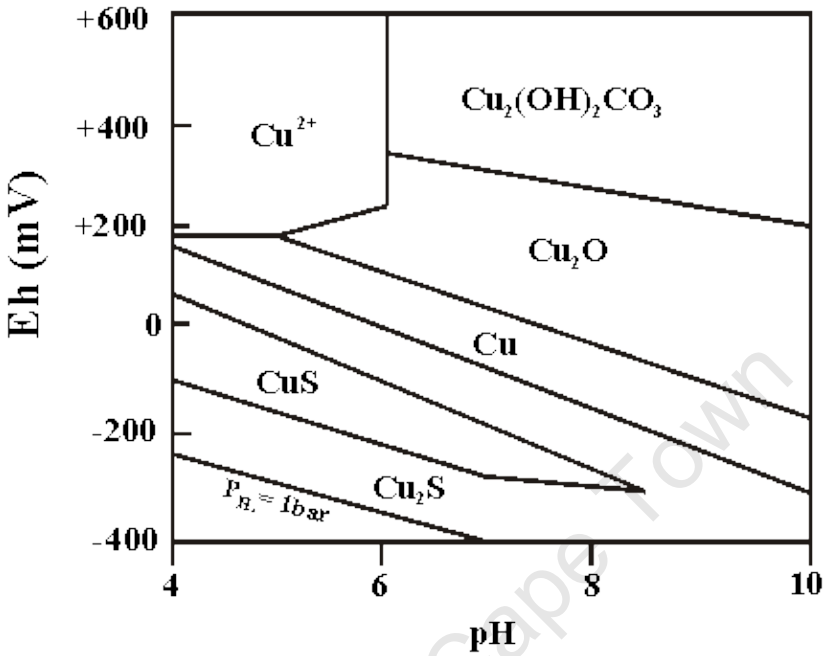

Figure 5.7: Cu-S-O Pourbaix diagram (Brookins, 1988)

In order to precipitate CuS as the dominant solid at an operating pH of 6, the Eh-pH diagram as shown in Figure 5.7 proposes an operating redox potential of not less than -200 mV but no higher than -100 mV. However, this determination is based on thermodynamic calculations and does not take reaction kinetics into account. The implication of this would be that the Pourbaix diagram assumes an infinite amount of time to attain the stable species and hence should only be used as a theoretical guideline. An important aspect that is highlighted by the Eh-pH diagram is that copper sulphide species are mostly stable in reducing conditions. The redox potential measured during the precipitation of CuS and shown in Figure 5.6 suggests predominantly oxidising conditions within the reactor. This implies that nitrogen sparging is inadequate as a means to create a fully inert and non-oxidising environment. Consequently, oxidation of precipitated CuS material cannot be fully inhibited. X-ray diffraction of the precipitate however confirms production of CuS, which is also consistent with covellite production by Mokone and co-workers (2012) under similar conditions.

Various techniques to reduce the oxidising conditions during metal sulphide precipitation have been employed. These include adding a small amount of Na_2SO_3 to water that has been sparged with nitrogen (Bebie, et al., 1998). The formation of Na_2SO_4 from Na_2SO_3 consumes 'all' the residual dissolved oxygen thereby reducing the oxidising conditions of the solution in the subsequent precipitation process. Another mechanism employed by Fornasiero and co-workers (1992) involved sparging argon gas instead of nitrogen. The use of nitrogen in this study was accepted, henceforth, as a systematic limitation. Zeta potential versus pH curves presented in subsequent sections will be used as a measure of the extent of oxidation.

5.2.2 Precipitation and partial oxidation of CuS particles

Copper sulphide precipitation experiments were carried out before the resultant precipitant particles were subjected to ζ-pH characterisation using a zeta-sizer auto-titrator. Three independent experiments were carried out and the results are presented as run 1, run 2 and run 3 in Figure 5.8. The pH range inclusive of all 3 runs was between a pH of 1.6 and 9 and the zeta potential range was between a maximum of -8 mV and a minimum of -51.1 mV.

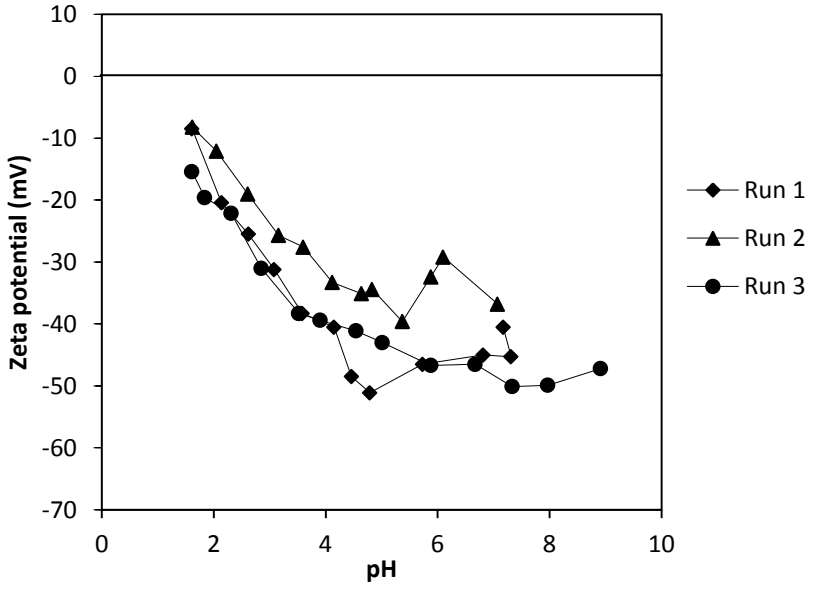

Figure 5.8: ζ-pH curve for CuS

By extrapolation, the iso-electric point of the precipitated CuS particles lies below a pH of 1.6 for all 3 runs. Electrokinetic studies on CuS by Mokone and co-workers (2010) predicted an iso-electric point of less than 2 while Liu and Huang (1992) predicted an iso-electric point of less than 1. This is consistent with the iso-electric point of less than 1.6 as predicted in this study. Experimental run 1 exhibited a global minimum at a pH of 4.8 and a zeta potential of -51.1 mV, run 2 at a pH of 5.4 and a zeta potential of -39.6 and run 3 at a much higher pH of 7.3 and a zeta potential of -50.1 mV. The global maxima for all 3 experimental runs were consistently at a pH of about 1.6 and for experimental run 1 and 2 this corresponded to a zeta potential of about -8 mV while a much lower value of -15.6 mV was observed for run 3. Run 1 and 3 exhibited good reproducibility between a pH of 2 and 4, but a deviation of up to 8 mV was observed at a pH of about 4.8 while the corresponding difference between run 1 and 2 is much higher. Compared to runs 1 and 3, run 2 consistently gave higher zeta potential values for corresponding pH values throughout the investigated pH spectrum and slight charge reversal behaviour was observed between a pH of 5 and 7. The general trend between runs 1 and 2 was similar and resulted in consistently lower zeta potential values with an increase in pH down to a minimum after which a slight increase in zeta potential was observed.

The ζ-pH characterisation of CuS particles after 30 minutes of oxidation is shown in Figure 5.9(a). The investigated pH range is between a pH of 1.5 and a pH of 8 and the zeta potential range is between a maximum of +2.57 mV and a minimum of -28.5 mV to give a difference of 31 mV. The CuS particles exhibit charge reversal behaviour with the existence of two iso-electric points between pH values of 7 and 7.6. The iso-electric point at low pH values can be obtained by extrapolation and this is consistently below a pH of 1.5 for all 3 experimental runs. A general trend exists between all 3 runs, a decrease in zeta potential with pH, down to a minimum after which the zeta potential begins to rise. The rate of zeta potential decrease with pH towards the global minimum is less steep than the rate of zeta potential increase with pH away from the global minimum. Good reproducibility exits between all the 3 runs except for the respective minima were the greatest difference measured is 10 mV between run 2 and run 3.

The metal sulphide particles exposed to 60 min of oxidation have the least difference between the measured global maximum and global minimum zeta potential values. The ζ-pH behaviour of the particles is shown in Figure 5.9(b) and is between a pH range of 1.6 and 8.2 while the difference in zeta potential between the global maximum and global minimum is about 24 mV.

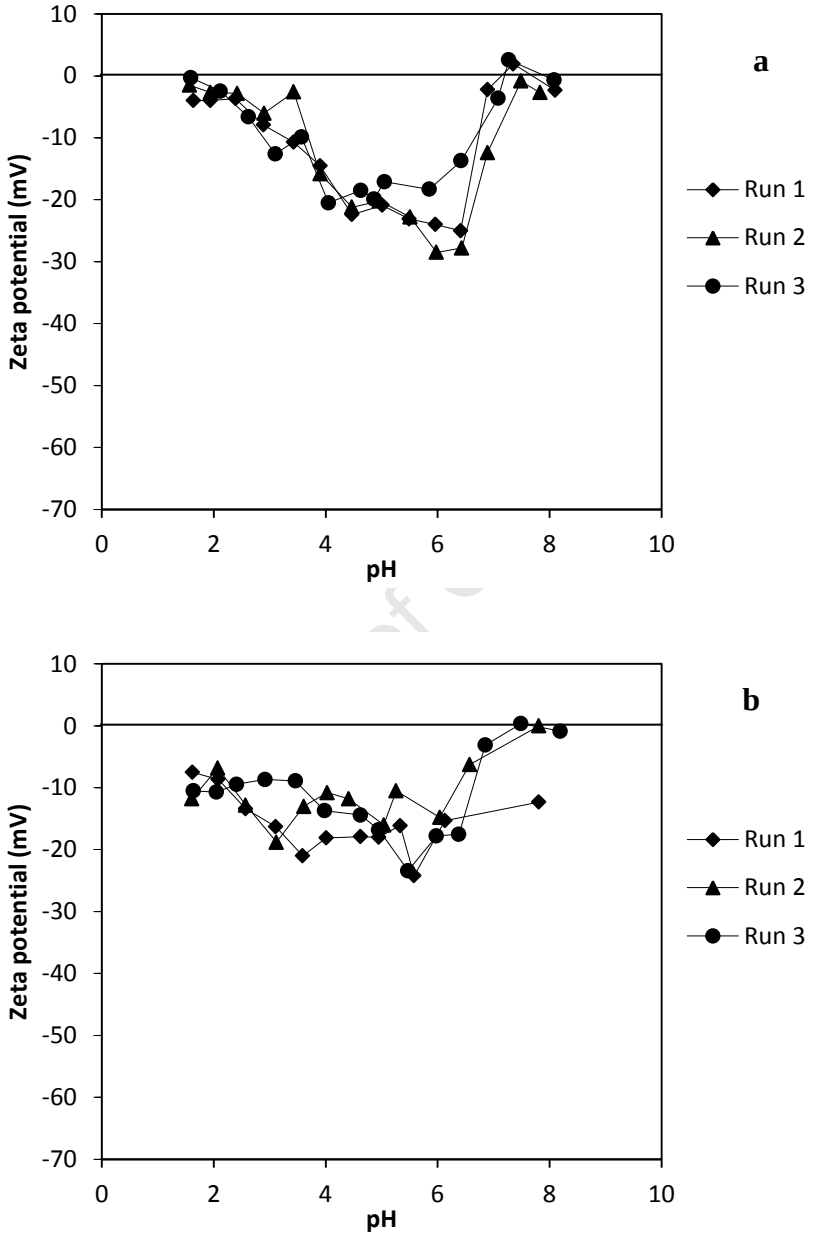

Figure 5.9: ζ-pH curves for CuS (a) after 30 min oxidation (b) after 60 min oxidation

Consequently, the change in zeta potential with pH is almost linear in the horizontal direction with the exception of higher pH values as observed for the experimental runs 2 and 3, where

an increase in zeta potential is observed. The local maximum at low pH is -7.5 mV and similar to that of the equivalent local maximum for the un-oxidised CuS particles but less than that of the CuS particles oxidised for 30 minutes.

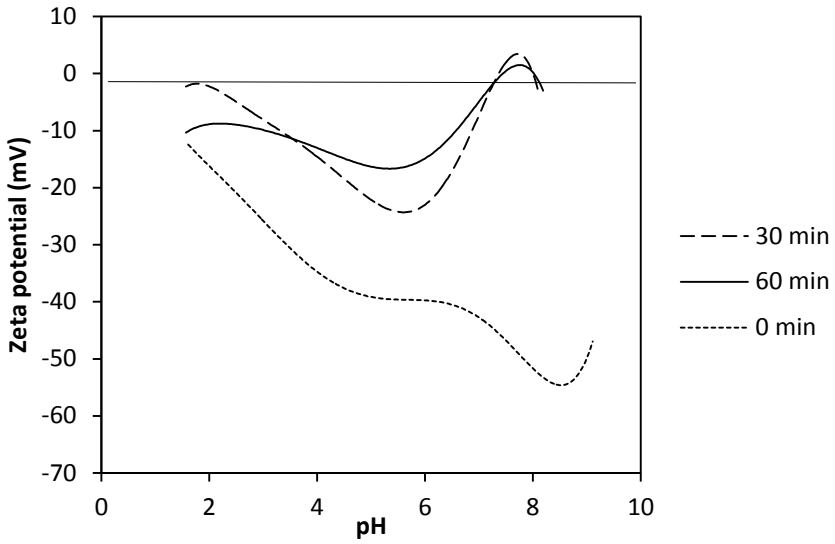

Figure 5.10: ζ-pH trend lines for all CuS particles

The observed overall trends are summarised in Figure 5.10 and show the change in the ζ-pH behaviour of the copper sulphide particles with an increase in oxidation. The trend lines were obtained by applying a mathematical line of best fit on the data points produced by all 3 runs for each time interval. It should also be noted that the ζ-pH behaviour of the copper sulphide particles conditioned in a basic medium then titrated toward acidic conditions was very similar, within experimental error, to that of particles conditioned in an acidic medium and then titrated towards basic conditions. A sample of results from both, acid to base and base to acid measurements are included as Appendix B.

Immediately after precipitation, the dissolved Cu^{2+} ion concentration is about 8 ppm which is a reduction of about 98.4 % from the initial synthetic Cu^{2+} ion waste stream concentration. With the progression of oxidation, the concentration of dissolved Cu^{2+} ions increases to a maximum of about 30 ppm. The first 30 min accounts for the dissolution of about 9.3 ppm Cu^{2+} ions while the subsequent 30 min accounts for about 12.8 ppm Cu^{2+} ions. The stated

results of the dissolved ion concentration with the extent of oxidation are shown in Figure 5.11.

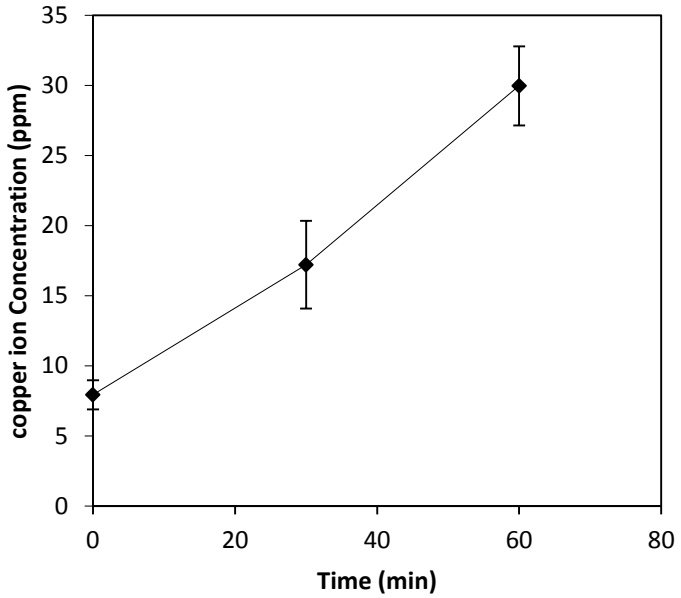

Figure 5.11: Concentration of dissolved copper with time of oxidation

5.3 Discussion

5.3.1 Precipitation of CuS particles under nitrogen

Work carried out by Healy and Moignard (1976) showed that a low iso-electric point most likely indicates a lightly oxidised or un-oxidised metal sulphide surface. This suggests that the precipitated CuS particles, in this study, can be considered as having undergone very minimal surface oxidation. Further to this, Dekkers and Schoonen (1994) stated that with significant oxidation leading to ion dissolution, charge reversal characteristics may be observed, implying the absence of it to be consistent with limited oxidation.

The ζ-pH behaviour exhibited by the CuS particles precipitated under nitrogen, as shown in Figure 5.8, is characteristic of the behaviour of some transition metal sulphides. As previously stated, the dominant species on the surface of a metal sulphide is the thiol group

(>S-H) and the observed decrease in zeta potential with an increase in pH is consistent with de-protonation of the thiol group. The rate of the respective zeta potential decrease with pH is dependent on the surface acidity constants. Experimental run 2 has consistently higher zeta potential values than both run 1 and 3. This is most likely due to possible oxygen contamination during experimental run 2 which is also confirmed by the charge reversal behaviour exhibited between a pH of 5 and 7 for the same run.

After optimising the model parameters to simulate the surface of CuS particles precipitated under nitrogen, a relatively good fit was obtained as shown in Figure 5.12. In this regard the simulated surface was considered to be representative of the surface of experimentally precipitated CuS particles before any induced oxidation. Experimental run 2 was not included in the model optimisation calculations because of the suspected partial oxidation.

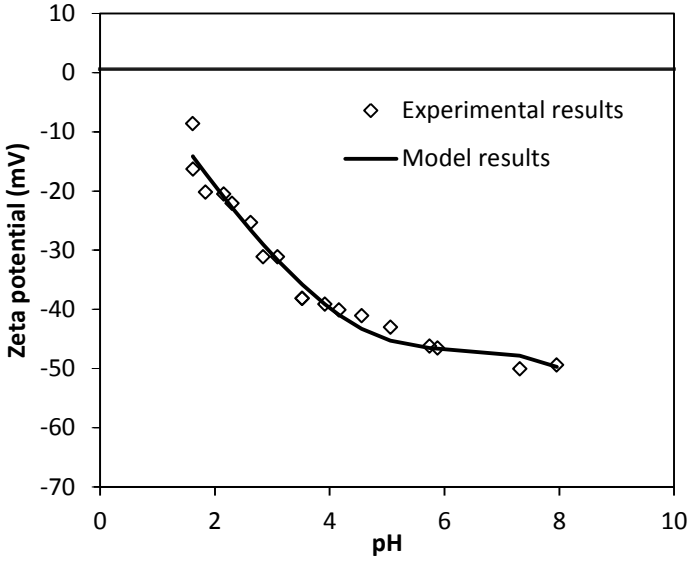

Figure 5.12: Model and experimental results of CuS particles precipitated under nitrogen

The surface of the CuS particles was consistent with the dominance of two surface sites:

A low coordination site, arbitrarily noted ‘i’, consistent with a sulphide group on a coordinately unsaturated lattice copper atom (>Cu-S-). The optimised acidity constants

suggested a moderately acidic site with a pKa_1 (>Cu-SH_2 / >Cu-SH_2^-) of -1.22 and a pKa_2 (>Cu-SH^- / >Cu-S^{2-}) of 10.0.

A high coordination site, arbitrarily noted 'v', consistent with a coordinately unsaturated lattice sulphide (>S-). The optimised acidity constants suggested a relatively more acidic site with a pKa_1 of -9.67 (SH_2^+ / >SH) and a pKa_2 (SH / $>S^-$) of 7.40.

Both sites had a surface density of 9.83, which was determined experimentally through crystallography work by Rosso and Hochella Jr (1999). The charges (>Cu-S^{2-}) and ($>S^0$) are governed by the crystal structure of CuS as described by (Pattrick, et al., 1997) The model Phreeqc input for the CuS particles at 0 min oxidation is included as Appendix C-1.

5.3.2 Post treatment of CuS particles under oxygen

With the respect to CuS particles precipitated under nitrogen, the zeta potential of CuS particles subjected to 30 min of oxidation increased throughout the investigated pH spectrum. The respective results are shown in Figure 5.9 and the observed trend is consistent with the partial substitution of the thiol groups (>S-H) with hydroxyl groups (>O-H). As hydroxyl groups are less acidic than thiol groups, the charge on the >OH is less negative than the charge on the >S-H, at identical pH. The rate of zeta potential change with pH for the 0 min curve and the 30 min curve, as shown in Figure 5.10, are very similar which may imply that the surface acidity constants of the thiol group remain unchanged. This would indicate and reinforce the notion that the thiol group in itself is not modified but only substituted from the surface and is also the basis of the modified CD-Music model.

In a model-based simulation of the surface of CuS, after 30 min of oxidation, it follows that depleting the number of thiol groups and replacing them with hydroxyl groups replicates the actual process of partial oxidation on the surface of CuS. This would entail that the number of hydroxyl groups on a partially oxidised surface would be equal to the number of depleted thiol groups. Therefore, the surface density of thiol groups on a partially oxidised surface of CuS would always be < 9.83 nm^2. Since the nature of the un-substituted thiol groups remain the same, their respective acidity constants should also remain the same. By iterating the density of the two sites, the thiol and the hydroxyl groups, it is theoretically possible to

replicate the ζ-pH behaviour of the CuS particles after 30 min of oxidation. A good model fit to the experimental data was obtained with the following optimised parameters:

Site 'i' has a density of 9.67 nm^{-2}

Site 'v' has a density of 9.30 nm^{-2}

Site 'j' is a hydroxyl group, that has replaced a thiol group initially occupying site 'i' and has a density of 0.16 nm^{-2}

Site 'o' is a hydroxyl group, that has replaced a thiol group initially occupying site 'v' and has a density of 0.53 nm^{-2}

The results of the surface complexation model are shown in Figure 5.13 and do not show the full pH range of the experimental data. A 'good' fit of the model to the experimental data was only possible up to pH 6, suggesting an additional mechanism other than thiol substitution by hydroxyl groups, beyond this pH. The Phreeqc model input for the CuS particles after 30 min oxidation and pH ≤ 6 is included as Appendix C-2

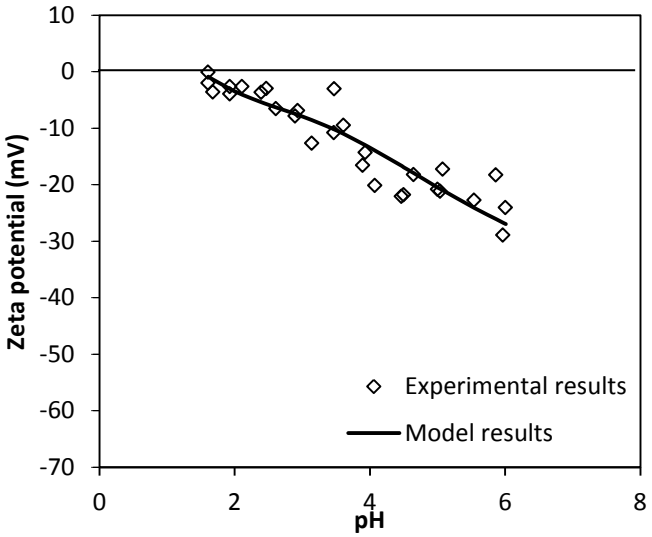

Figure 5.13: Model and experimental data of CuS after 30 min oxidation

The CuS particles oxidised for 30 min exhibit charge reversal properties at a pH ≥ 6 which, according to Nicolau and Menard (1991), is synonymous with the specific adsorption of hydrolysable dissolved metal ion species. To confirm an increase in metal ion activity, the

concentration of dissolved metal ions after oxidation is shown in Figure 5.11. A steady increase in the concentration of dissolved metal ions is measured with an increase in oxidation. Consequently the CuS particles having undergone partial oxidation are suspended in a solution of increased metal ion activity and this may affect the electrical double layer and hence zeta potential in two different ways. Firstly an increase in the ionic activity constricts the electrical double layer and this can be responsible for a decrease in the magnitude of the surface charge potential. In the case of negatively charged particles an increase in the zeta potential will be observed. The observed increase in zeta potential however is too large to be solely attributed to electrical double layer compression, taking into account the increase in the magnitude of ionic activity. It should also be noted that this phenomena does not generally result in charge reversal.

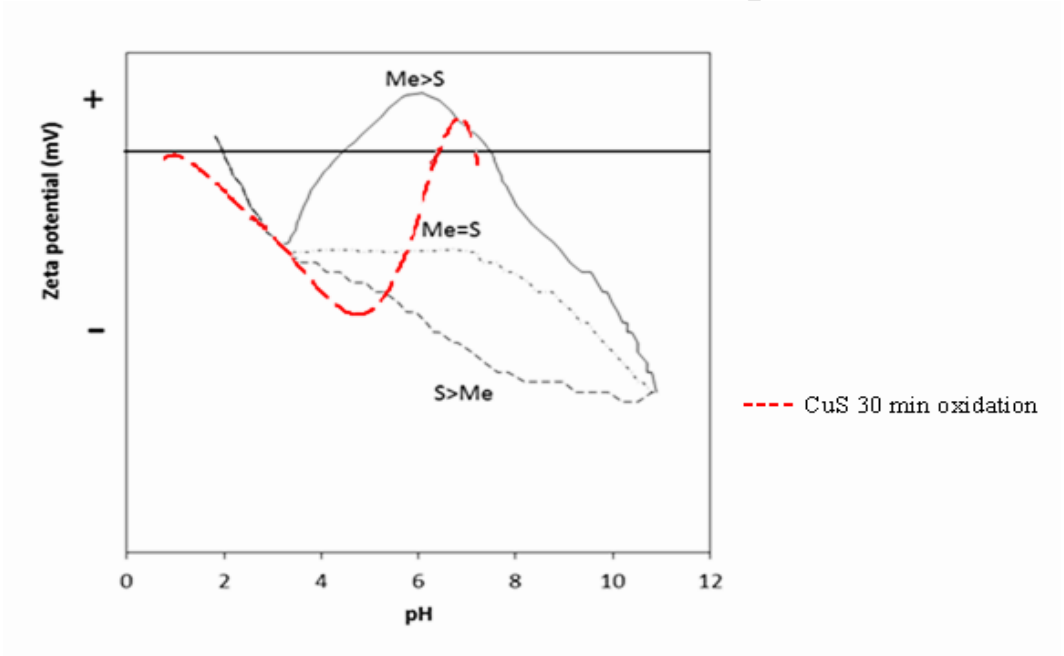

Figure 5.14: Effect metal to sulphide ratio on zeta potential

Additionally some authors postulate that if the concentration increase is isolated to the lattice ions then specific adsorption of such ions on to the surface Bronsted sites can occur (Guindo, et al., 1996). The net change in zeta potential would then depend on the ratio between the increase in metal ions and that of the sulphide ions. Dekkers and Schoonen (1994) presented the general effect of the ratio between lattice ions on the ζ-pH properties of metal sulphides,

the results are shown in Figure 5.14. By aligning the position of the iso-electric points the ζ-pH curve for the CuS particles after 30 minutes of oxidation can be superimposed on the results presented by Dekkers and Schoonen (1994). The CuS curve is very similar in shape to the curve representing a system with an excess of metal ions.

Metal ions are readily hydrolysed in solution and form various aqueous species, whose concentration is pH dependent. Figure 5.15 shows the speciation diagram of copper species in solution at a concentration of 0.3 ppm, as computed by Faur-Brasquet and co-workers (2002). Up to a pH of about 6, the dominant copper species in solution is the Cu^{2+} ion. Lyklema (1976) stated that, in the event of specific adsorption of ions a shift in the iso-electric point would be observed in relation to the same system in the absence of specific adsorption. Figure 5.14 represents 3 different systems that have the following dominant solution chemistry with respect to metal and sulphide ions; excess metal ions, equi-molar, and excess sulphide ions. The fact that all 3 systems converge on the same iso-electric point suggests that, according to Lyklema (1976), specific adsorption of metal lattice ions is not prominent. The rise in zeta potential with an increase in pH can then be attributed to the adsorption of the respective hydrolysed species as they become stable.

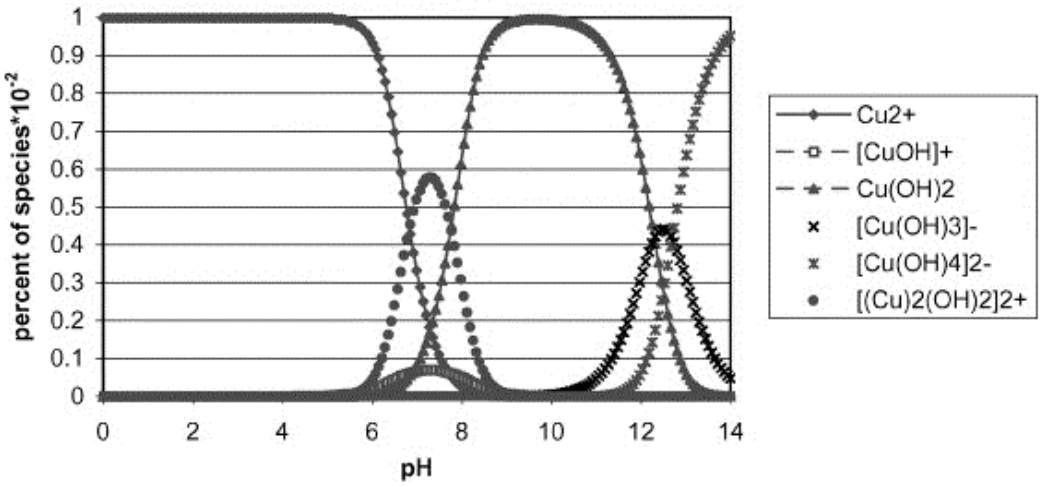

Figure 5.15: Copper speciation diagram (Faur-Brasquet et al., 2002)

The sharp increase in zeta potential of CuS particles observed around a pH of 6 (Figure 5.9) is most likely due to the adsorption of $CuOH^+$ on the surface of the particles. A strong correlation exists between the increase in zeta potential of the CuS particles and an increase in the activity of copper hydroxide species in solution at a pH of 6, as shown in Figure 5.15. This is also consistent with thermodynamic calculations by Kesler (1989) that show copper hydroxide as being unstable at pH values below 6 in mineral sulphide solutions.

In order to model the full spectrum of the investigated pH, it is necessary to account for the complexation of the $CuOH^+$ species for pH values greater than 6. This is because the observed change in zeta potential is not only due to the substitution of surface thiol groups but also adsorption of the hydroxide species. By keeping constant all the formerly determined parameters applied for the surface complexation model of CuS particles partially oxidised for 30 min, an additional adsorption component of $CuOH^+$ was added to the model. The results of the optimised model, giving the full experimental pH range are shown in Figure 5.16.

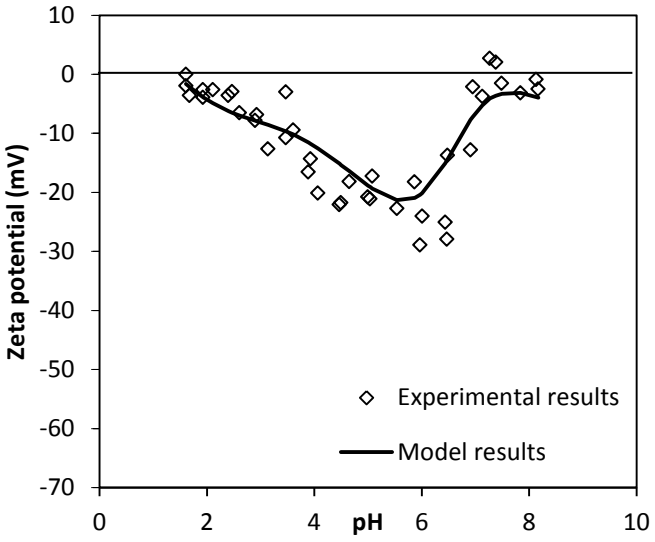

Figure 5.16: Optimised model results, including $CuOH^+$ complexation, compared to experimental results for CuS particles after 30 min oxidation

The association constants in the optimised model were:

low coordination $>Cu\text{-}SH^- + CuOH+ = >Cu\text{-}SH\text{-}CuOH$, $\log_{10}(k) = 2.36$

high coordination $>SH^{+} + CuOH+ = >SH\text{-}CuOH^{2+}$, $\log_{10}(k) = 2.30$

low coordination $>Cu\text{-}OH^{-} + CuOH+ = >Cu\text{-}OH\text{-}CuOH$, $\log_{10}(k) = 3.13$

high coordination $>OH^{+} + CuOH+ = >OH\text{-}CuOH^{2+}$, $\log_{10}(k) = 2.36$

A better fit was obtained considering outer sphere complexation than considering inner sphere complexation. The Phreeqc model input code for the CuS particles at 30 min oxidation, full pH range, is included as Appendix C-3.

After 60 min of oxidation the CuS particles seem to show less sensitivity to pH up to about neutral conditions, this is consistent with H^{+} ions becoming less prominent potential determining ions. On the surface of an un-oxidised CuS particle it is the thiol group that is receptive to H^{+} ions and an increased substitution of this group by the hydroxyl group may be responsible for the observed trend shown in Figure 5.9.The concentration of Cu^{2+} ions after 60 min of oxidation is about 30 ppm, an increase from a concentration of about 17 ppm after 30 min of oxidation. This clearly suggests increased oxidative dissolution of Cu^{2+} ions and the associated effects on zeta potential. As Cu^{2+} ions are liberated by the surface they increase the number of exposed surface thiol groups. This increases the number of thiol groups that can be replaced by the hydroxyl group and therefore the magnitude of the zeta potential increase with oxidation. The effects of an increase in the ionic strength between particles oxidised for 30 min and those oxidised for 60 min by constriction of the electrical double layer may be insignificant to account for the changes in the associated ζ-pH behaviour but may have a contributory effect. On the other hand, an increase in solution species may result in their respective oxidation and subsequent adsorption of the oxidation products on to the surface of the CuS particles which may lead to the observed ζ-pH behaviour. The increase in zeta potential observed around a pH of 6 may be still due to the adsorption of copper hydroxide species as previously suggested.

Modelling of the surface of CuS particles after 60 min of oxidation was not carried out because the experimentally produced ζ-pH behaviour of the particles seems to suggest surface transformation not consistent with solely substitution of thiol groups by hydroxyl groups.

5.3.3 Effect of partial oxidation on settling

Lyklema (1976) stated that difficulties in conducting research into colloid stability arise due to the fact that it is difficult to change only one variable at a time. This is specifically the case when it comes to partial oxidation, since not only is the nature of the metal sulphide particles surface modified, but also the solution chemistry. The combined effect of these changes may induce a hydrophilic or hydrophobic nature on the surface of the metal sulphide particles and this can cause deviation from the DLVO theory. In order to ascertain the settling nature of CuS particles having undergone partial oxidation, settleability results together with the associated particle zeta potential are shown in Figure 5.17.

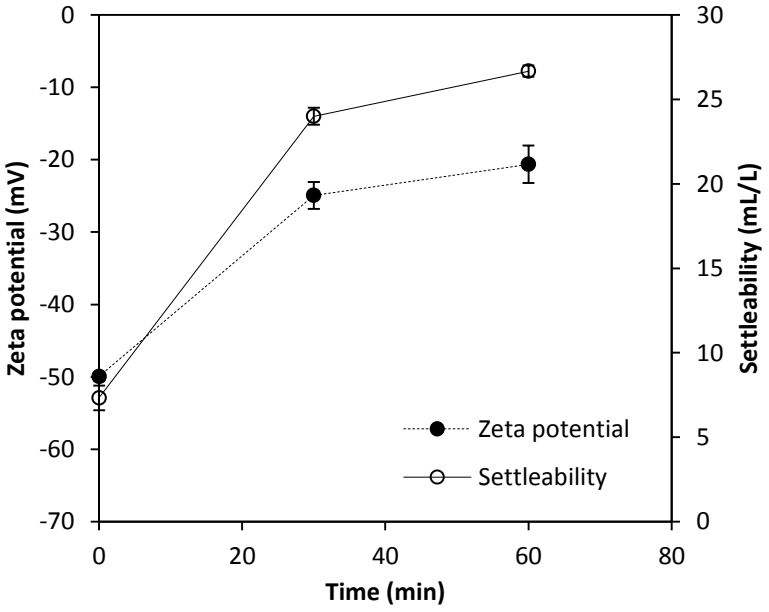

Figure 5.17: Settleability of CuS particles at different extents of oxidation

All zeta potential measurements given were at a constant pH value of 6. The initial settleability of the CuS particles before any induced oxidation was about 7 mL/L increasing to about 24 mL/L after 30 min of oxidation and then to a maximum of about 27 mL/L after 60 min of oxidation. The zeta potential of the CuS particles was about -50 mV before any oxygen sparging, increasing to about -25 mV after 30 min of oxidation and then attained a maximum of about -21 mV after an hour of oxidation.

The results presented in Figure 5.17 show a clear trend relating settleabilty with zeta potential. As the zeta potential increases (decreases in magnitude), settleability increases. Decreasing zeta potential is consistent with decreasing the inter-particle electrostatic forces, which are repulsive in nature and this promotes aggregation. This is consistent with the observed trend in Figure 5.17 and implies that the CuS particles exposed to partial oxidation treatment obey the DLVO theory.

The associated DLVO profiles of CuS particles under nitrogen and those exposed to 30 min and 60 min of oxidation are shown in Figure 5.19 to 5.20 respectively. Prior to any oxidation, the maximum energy barrier between colliding CuS particles is around 2.44 kT. This energy barrier is associated with a settleability of about 7 mL/L. In order to improve settleability, the electrostatic repulsion of particles has to be reduced. For particles that obey the DLVO theory, this is possible by reducing the zeta potential of the associated particles. As the zeta potential of particles approaches zero, the interaction curve (Net total) approaches the van der Waals curve and the particles involved attract each other at any separation distance. As shown in Figure 5.19 and 5.20, partial oxidation of CuS particles induces this kind of behaviour which results in rapid coagulation of the particles.

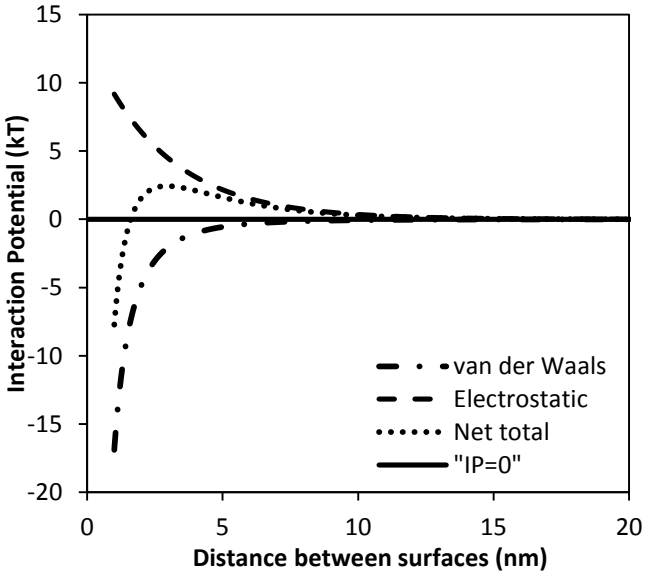

Figure 5.18: DLVO profile of CuS particles before oxidation

The increase in settleability observed between particles partially oxidised for 30 min and those for 60 min was not significant and this could be due mainly to the fact that at both conditions, attraction was the dominant inter-particle force. This implies that, it may not be necessary to expose CuS particles to an hour of oxidation in order to induce settling, as the gain, with respect to improved settleability may be compromised by the loss due to Cu^{2+} ion dissolution.

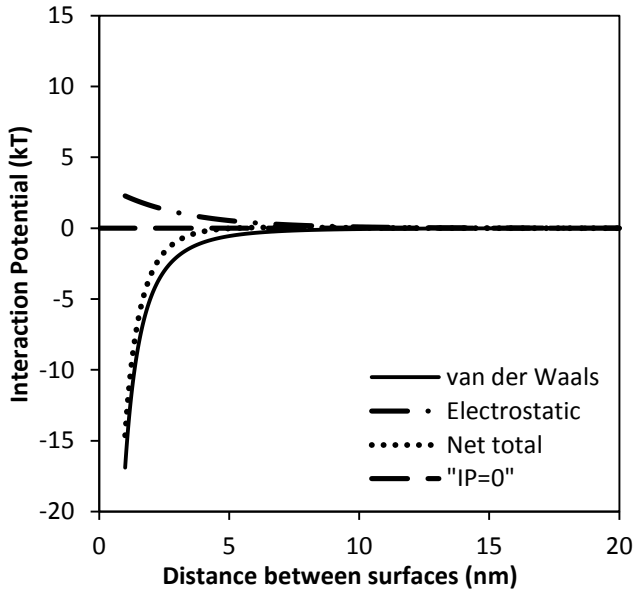

Figure 5.19: DLVO profile of CuS particles after 30 min of oxidation

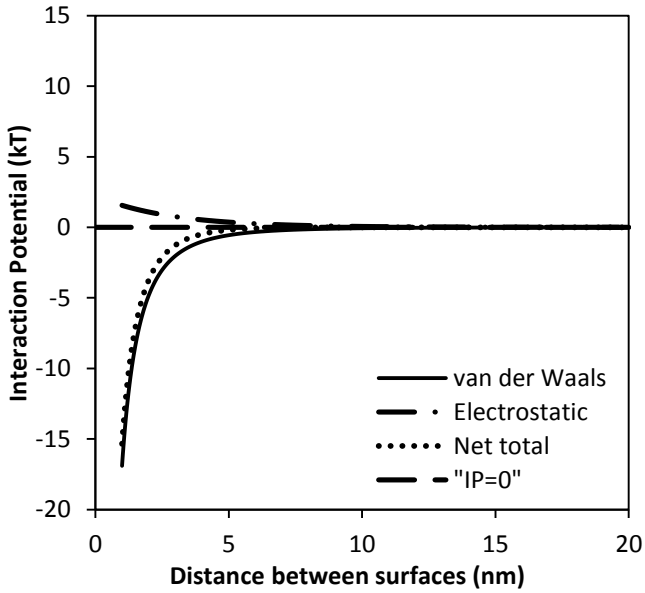

Figure 5.20: DLVO profile of CuS particles after 60min of oxidation

A reduced period of oxidation may also have financial benefits, as it reduces the amount of oxygen sparged, while a lesser residence time is beneficial if the technique is to be used for the treatment of large volumes of CuS suspensions.

6 Conclusions and recommendations

6.1 Conclusions

6.1.1 Effect of lattice ions on settling characteristics of CuS

The criteria for accepting or rejecting a potential treatment process as being a viable option in improving the solid-liquid separation properties for a CuS suspension was based on the process not exceeding a dissolved Cu^{2+} ion concentration of 5 % the initial metal ion concentration. After the precipitation of CuS a dissolved Cu^{2+} ion concentration of 7.33 mg/L is measured, by addition of 15 mg/L of Cu^{2+} ions the copper ion solution concentration should rise to about 22.3 mg/L which represents 4.46 % of the initial metal ion concentration. Settleability increases by a factor of 2.4 to 17.7 mL/L, which together with the acceptable amount of dissolved metal ions makes this treatment process viable in alleviating solid-liquid separation challenges during copper sulphide precipitation. Settleability of CuS particles with suspension in a solution of 25 mg/L of Cu^{2+} ions increases to a maximum of about 21 mL/L, an increase by a factor of 2.9. However, the process is rendered unsustainable due to a combined Cu^{2+} ion concentration of 32.3 mg/L (25 mg/L + 7.3 mg/L), 1.46 % above the set percentage threshold.

Although the current work cannot give insight into the actual mechanism involved for lattice ion incorporation to the electrical double layer, it clearly shows that, in addition to the protonation of surface species, sulphide and copper ions are also potential determining ions. It can be further concluded that within the range of the experimental conditions, an increase in the concentration of dissolved copper ions increases the zeta potential (less negative) of CuS particles while an increase in the concentration of dissolved sulphide ions has the opposite effect. It remains very difficult to account for all inter-particle forces that exist in a suspension and as such it will be stated that, to a larger extent CuS particles obey the DLVO theory.

6.1.2 Effect of partial oxidation on settling characteristics of CuS

The surface of the copper sulphide particles precipitated under nitrogen was consistent with minimal oxidation due to the predicted low isoelectric point. These particles had a relatively low settleability of about 7 mL/L. For the CuS particles after 30 min of partial oxidation, the nature of the surface was consistent with one for one substitution of surface thiol groups with hydroxyl groups up to a pH of 6. Beyond this pH two mechanisms seemed to dictate the charge development on the surface of CuS particles. Substitution of thiol groups was coupled with the adsorption of hydrolysed copper hydroxide compounds, and this was supported by the successful modelling of the respective CuS surface using the modified CD-Music model. As the extent of oxidation was increased, the dissolved Cu^{2+} ion concentration also increased but still fell below the set threshold concentration of 5%. Settleability of the respective CuS particles was greatly improved and this was attributed to the promotion of aggregation due to the reduction of particle electrostatic repulsions. This suggested that the CuS particles after 30 min of oxidation obeyed the DLVO theory and, therefore, the technique can be used as a successful means in improving the settling properties of precipitated CuS particles.

After 60 min of partial oxidation, settleability of the CuS was greatly improved by a factor of up to 3.8. However, the dissolved Cu^{2+} ion concentration was above the set threshold of 25 mg/L and hence this rendered the technique 'unsustainable'. The dominant mechanism of oxidation, after 60 min of partial oxidation, could not be inferred from the results, but it was postulated that it involved both thiol substitution by hydroxyl groups and also the adsorption of both, hydrolysed and solution oxidation products. Non DLVO behaviour was not observed up to 60 min of oxidation, a DLVO profile showed a reduction in electrostatic potential which translated to an increase in the aggregation behaviour of the CuS particles, observed as an increase in settleability.

6.2 Overall conclusions

Both of the mechanisms that were employed in trying to improve the settling properties of precipitated CuS particles, proved to be successful to varying extents. The use of partial oxidation, as a post-precipitation treatment process was, however, relatively more efficient in improving the settling properties, with respect to the concentration of dissolved Cu^{2+} ions. It can also be concluded that, within the experimental range of conditions, CuS particles largely obey the DLVO theory. A choice between the two processes would, however, depend on the exact nature, properties of the waste water stream and available resources.

6.3 Recommendations

Although both the post precipitation treatment methods investigated in this study showed reasonable success in alleviating the solid-liquid separation challenges that compromise metal sulphide precipitation, further research may need to be carried out before any practical implementation. In most industrial and mine waste, a mixture of ions exist at varying concentrations, thus it may be necessary to further this work by investing the effect of different ions on the relative effectiveness of the methods tested in the current study.

During partial oxidation treatment of the CuS particles, 'pure' oxygen was sparged into a batch reactor in order to allow the necessary surface changes, favourable to inducing settling, to occur. In order for this technique to become widely accepted, it is generally a pre-requisite that it should be simple and be associated with a minimal financial cost. Consequently, it may be necessary to investigate the effectiveness of using air as a source of oxygen in order to partially oxidise the surface of the CuS particles. However, the use of air may require a longer residence time than that of using oxygen, to achieve the same effects. As such, the effect of improving mass transfer of oxygen in the air to the liquid would need to be investigated, with respect to energy input and residence time of the suspended CuS particles in the sparged vessel.

7 References

Bebie, J., Schoonen, M. A., Fuhrmann, M. & Strongin, D. R., 1998. Surface charge development on transition metal sulfides: An electrokinetic study. *Geochemica et Cosmochimica Acta,* 62(4), pp. 633-642.

Benner, S. G., Blowes, D. W., Ptacek, C. J. & Mayer, K. U., 2002. Rates of sulfate reduction and metal sulfide precipitation in a permeable reactive barrier. *Applied Geochemsitry,* 17(3), pp. 301-320.

Bijmans, F. M. M., van Helvoort, P.-J., Buisman, C. J. N. & Lens, P. N. L., 2009. Effect of the sulfide concentration on zinc bio-precipitation in a single stage sulfidogenic bioreactor at pH 5.5. *Separation and Purification Technology,* Volume 69, pp. 243-248.

Blais, J. F., Dufresne, S. & Mercier, G., 1999. State of the art of the technological development from metal removal from industrial effluents. *Journal of Water Science,* 12(4), pp. 689-713.

Boonstra, J. et al., 1999. Biological treatment of acid mine drainage: Biohydrometallurgy and the Environment Toward the Mining of the 21st Century Proceedings of the International Biohydrometallurgy Symposium. *Process Metallurgy,* Volume 9, pp. 559-867.

Brookins, D. G., 1988. *Eh-pH diagrams for geochemistry.* New York: Springer-Verlag.

Butler, I. B., Schoonen, M. A. A. & Rickard, D. T., 1994. Removal of dissolved oxygen from water: A comparison of four common techniques. *Talanta,* 41(2), pp. 211-215.

Chander, S., 1991. Electrochemistry of sulfide flotation:Growth characteristics of surface coatings and their properties, with special reference to chalcopyrite and pyrite. *International Journal of Mineral Processing,* 33(1-4), pp. 121-134.

Chapman, D. L., 1913. A contribution to the theory of electrocapillarity. *The Philosophical Magazine,* Volume 25, pp. 475-481.

Charerntanyarak, L., 1999. Heavy metals removal by chemical coagulation and precipitation. *Water Science Technology,* 39(10-11), pp. 135-138.

Charlton, S. R. & Parkhurst, D. L., 2011. Modules based on the geochemical model PHREEQC for use in scripting and programming languages. *Computers and Geosciences,* 37(10), pp. 1653-1663.

Dekkers, J. M. & Schoonen, M. A. A., 1994. An electrokinetic study of synthetic greigite and pyrrhotite. *Geochimca et Cosmochimica,* 58(19), pp. 4147-4153.

Deryagin, B. V. & landau, L., 1941. Theory of the stability of strongly charged lyophobic sols and of the adhesion of strongly charged particles in solutions of electrolytes. *Acta Physicochimica,* Volume 14, pp. 633-662.

DiFeo, A., Finch, J. A. & Xu, Z., 2001. Sphalerite-silica interactions: effect of pH and calcium ions. *International Journal of Mineral Processing,* Volume 61, pp. 57-71.

Duran, J. D. G., Guindo, M. C. & Delgado, A. V., 1995. Stability of monodisperse zinc sulphide colloidal dispersions. *Langmuir,* 11(10), pp. 3648-3655.

Dyer, J., Scrinver, N. C. & Dentel, S. K., 1998. A practical guide for determining the solubility of metal hydroxides and oxides in water. *Environmental Progress,* 17(1), pp. 1-8.

Everett, D. H., 1988. *Basic Principles of Colloid Science.* London: Royal Society of Chemistry.

Faur-Brasquet, C., Reddad, Z., Kadirvelu, K. & Le Cloirec, P., 2002. Modelling the adsorption of metal ions (Cu2+, Ni2+, Pb2+) onto ACCs using surface complexation models. *Applied Surface Science,* 196(1-4), pp. 356-365.

Fornasiero, D., Eijt, V. & Ralston, J., 1992. An electrokinetic study of pyrite oxidation. *Colloids and Surfaces,* 62(1-2), pp. 63-73.

Fullston, D., Fornasiero, D. & Ralston, J., 1999. Zeta potential study of the oxidation of copper sulphide minerals. *Colloids and Surfaces,* Volume 146, pp. 113-121.

Gouy, M., 1910. Sur la constitution de la charge électrique a la surface d'un electrolyte. *Journal of physics,* Volume 9, pp. 457-468.

Grasso, D. et al., 2002. A review of non-DLVO interactions in environmental colloidal systems. *Environmental Science and Bio/Technology,* Volume 1, pp. 17-38.

Guindo, M. C., Zurita, L., Duran, J. D. G. & Delgado, A. V., 1996. Electrokinetic behaviour of spherical colloidal particles of cadmium sulphide. *Materials Chemistry and Physics,* Volume 44, pp. 51-58.

Guy, P. J. & Trahar, W. J., 1985. The effects of oxidation and mineral interaction on sulfide flotation. *Flotation of Sulfide Minerals, ed., K.S.E. Forssberg, Elsevier,* pp. 61-79.

Hammack, R. W., Dvorak, D. H. & Edenborn, H. M., 1993. *The use of biogenic hydrogen sulfide to selectively recover copper and zinc from severely contaminated mine drainage.* Warrendale, The Minerals, Metals and Materials Society, pp. 631-639.

Hartel, R. W., Gottung, B. E., Randolph, A. D. & Drach, G. W., 1986. Mechanisms and kinetic modelling of calcium oxalate crystal aggregation in a urinelike liquor. Part I. Mechanisms. *American Institute of Chemical Engineers,* 37(7), pp. 1176-1185.

Healy, T. W. & Moignard, M. S., 1976. A review of electrokinetic studies of metal sulphides. Volume 1, p. 275.

Helmholtz, H., 1879. Studies of electrical interfaces. *Annalen Der Physik Und Chemie,* 243(1879), pp. 337-382.

Hiemstra, T., Van Riemsdijk, W. H. & Bolt, G. H., 1989. Multisite proton modeling at the solid/solution interface of (hydr)oxides: A new approach: I. Model description and evaluation of intrinsic reaction constants. *Journal of Colloid and Interface Science,* Volume 133, pp. 91-104.

Horzempa, L. M. & Helz, G. R., 1979. Controls on the stability of sulfide sols: colloidal covellite as an example. *Geochimica et Cosmochimica Acta,* Volume 43, pp. 1645-1650.

Hunter, R. J., 1986. *Foundations of Colloid Science Volume 1.* New York: Oxford University Press.

Israelachvili, J., 1992. *Intermolecular and surface forces.* 2nd ed. London: Academic Press.

Jones, A. G., Hostomsky, J. & Wach, S., 1996. Modelling and analysis of particle formation during agglomerative formation during agglomerative crystal precipitation processes. *Chemical EngineeringCommunications,* 146(1), pp. 105-130.

Kaksonen, A. H., Riekkola-Vanhanen, M. L. & Puhakka, J. A., 2003. Optimization of metal sulphideprecipitation in fluidized-bed treatment of acidic wastewater. *Water Research*, 37(2), pp. 255-266.

Karbanee, N., van Hille, R. P. & Lewis, A. E., 2008. Controlled nickel sulfide precipitation using gaseous hydrogen sulfide. *Industrial and Engineering Chemistry Research* , Volume 47, pp. 1596-1602.

Karpinski, P. H. & Wey, J. S., 2002. Precipitation Processes. In: A. S. Myerson, ed. *Hand Book of Crystallization.* Woburn: Butterworth-Heinmann, pp. 141-159.

Kelebek, S. & Smith, G. W., 1989. Electrokinetic properties of a galena and chalcopyrite with the collectroless flotation. *Colloids and Surfaces,* Volume 40, pp. 137-143.

Lewis, A. E., 2006. Fines formation (and prevention) in seeded precipitation processes. *Kona,* Volume (Invited contribution), pp. 119-125.

Liu, J. C. & Huang, C. P., 1992. Electrokinetic characteristics of some metal sulfide-water interfaces. *Langmuir,* Volume 8, pp. 1851-1856.

Lyklema, J., 1976. Lyophobic sol stability in mixed media. *Pure and Applied Chemistry,* Volume 48, pp. 449-455.

Marchioretto, M. M., Bruning, H. & Rulkens, W., 2005. Heavy metals precipitation in sewage sludge. *Separation Science Technology,* 40(16), pp. 3393-3405.

Mersmann, A., 1999. Crystallisation and Precipitation. *Chemical Engineering and Processing: Process Intensification,* 38(4-6), pp. 345-353.

Mersmann, A., 2001. *Crystallization Technology Handbook.* 2nd ed. New York: Marcel Dekker.

Mirnezami, M., Restrepo, L. & Finch, J. A., 2003. Aggregation of spalerite: role of zinc ions. *Journal of Colloid and Interface Science,* Volume 259, pp. 36-42.

Mokone, T. P., van Hille, R. P. & Lewis, A. E., 2010. Effect of solution chemistry on particle characteristics during metal sulphide precipitation. *Journal of Colloid and Interface Science,* Volume 351, pp. 10-18.

Mokone, T. P., van Hille, R. P. & Lewis, A. E., 2012. Effect of post-precipitation conditions on surface properties of colloidal metal sulphide precipitates. *Hydrometallurgy,* Volume 119-120, pp. 55-66.

Mokone, T. P., van Hille, R. P. & Lewis, A. E., 2012. Metal Sulphides from waste-water: Assessing the impact of supersaturation control strategies. *Water Research,* 46(7), pp. 2088-2100.

Mullin, J. W., 1972. *Industrial Crystallization.* London: Butterworth.

Mullin, J. W., 2001. *Crystallization.* 4th ed. Oxford: Butterworth-Heinemann.

Muster, T. H. & Prestidge, C. A., 1995. Rheological investigations of sulphide mineral slurries. *Minerals Engineering,* 8(12), pp. 1541-1555.

Nicolau, Y. F. & Menard, J. C., 1991. An electrokinetic study of ZnS and CdS surface chemistry. *Journal of Colloid and Interface Science,* 148(2).

Nortier, P., Borosy, A. P. & Allavena, M., 1997. Ab initio hartree-fock study of Bronsted acidity at the surface of oxides. *Journal of Physical Chemistry,* 101(8), pp. 1347-1354.

Ottewill, R. H., 1982. Concentrated dispersions. *Chemical Society Review Symposium Ed. J. W. Goodwin, Royal Society of Colloidal Dispersions,* pp. 197-217.

Overbeek, J. T. G., 1977. Recent developments in the understanding of colloid stability. *Journal of Colloidal Interface Science,* 2(58), pp. 408-422.

Pashley, M. R. & Karaman, E. M., 2004. *Applied Colloid and Surface Chemistry.* Chichester: John Wiley and Sons.

Pattrick, R. A. D. et al., 1997. The structure of amorphous copper sulphide precipitates: An X-ray absorption study. *Geochimica et Cosmochimica Acta,* 61(10), pp. 2023-2036.

Peters, R. W., Ku, Y. & Batthacharyya, D., 1984. Evaluation of recent treatment techniques for removal of heavy metals from industrial wastewaters. *AIChE Meeting,* pp. 19-22.

Reerink, H. & Overbeek, J. G., 1954. The rate of coagulation as a measure of the stability of silver iodide sols. *Discussions of the Faraday Society,* Issue 18, pp. 74-84.

Sampaio, R. M. M. et al., 2010. Zn-Ni sulfide selective precipitation: The role of supersaturation. *Separation and Purification Technology,* 74(1), pp. 108-118.

Schlauch, R. M., 1978. *Colloid free precipitation of heavy metal sulfides.* USA, Patent No. 4102784.

Shaw, D. J., 1970. *Introduction to colloid and surface chemistry.* London: Butterworths.

Smart, R. S. C. et al., 1998. Surface analytical studies of oxidation and colletor adsorption in sulphide mineral flotation. *Scanning Microscopy,* 12(4), pp. 553-583.

Söhnel, O. & Garside, J., 1992. *Precipitation: basic principles and industrial applications.* Oxford: Butterworth-Heinemann.

Söhnel, O., Mullin, J. W. & Jones, A. G., 1988. Crystallization and agglomeratio kinetics in a batch precipitation of strontium molybdate. *Industrial & Engineering Chemistry Research,* 27(9), pp. 1721-1728.

Stachowicz, M., Hiemstra, T. & van Riemsdijk, W. H., 2006. Surface speciation of As(iii) and As(V) inrelation to charge distribution. *Journal of Colloid and Interface Science,* 302(1), pp. 62-75.

Utgikar, V. P. et al., 2002. Inhibition of sulfate-reducing bacteria by metal sulfide formation in bioremediation of acid mine drainage. *Environmental Toxicology,* 17(2002), pp. 40-48.

van Hille, R. P., Peterson, A. K. & Lewis, A. E., 2005. Copper sulphide precipitation ina fluidised bed reactor. *Chemical Engineering Science,* 60(10), pp. 2571-2578.

Veeken, A. H. & Rulkens, W. H., 2003. Innovative developments in the selective removal and reuse of heavy metals from wastewaters. *Water Science and Technology,* 47(10), pp. 9-16.

Vergouw, J. M., Difeo, A., Xu, Z. & Finch, J. A., 1998. An agglomeration study of sulphide minerals using zeta potential and settling rate. Part 2: Sphalerite/pyrite and sphalerite/galena. *Minerals Engineering,* 11(7), pp. 605-614.

Vergouw, J. M., Difeo, A., Xu, Z. & Finch, J. A., 1998. An agglomeration study of sulphide minerals using zeta-potential and settling rate. Part 1: pyrite and galena. *Minerals Engineering,* 11(2), pp. 159-169.

Verwey, E. J. & Overbeek, J. T. G., 1948. *Theory of the stability of lyophobic colloids.* New York: Elsevier.

Williams, R. & Labib, M. E., 1985. Zinc sulphide surface chemistry: an electrokinetic study. *Journal of Colloid and Interface Science*, 106(1).

Appendices

Appendix A

Example of raw data: effect of lattice ions on zeta potential and settleability.

Zeta potential analysis (3 measurements per sample for 3 independent runs)

Mass of S^{2-} added (mg/L)	**Zeta potential measurements (mv)**											
	Run 1				Run 2				Run 3			
	1	2	3	**Avge**	1	2	3	**Avge**	1	2	3	**Avge**
0	-49.4	-52	-50.9	**-50.8**	-50.7	-51.5	-48.7	**-50.3**	-48.9	-50.3	-47.3	**-48.7**
7	-55.2	-57.3	-56.1	**-56.2**	-59.3	-59.4	-58	**-58.9**	-55.1	-57.3	-57.1	**-56.5**
12	-56.9	-57.9	-57.1	**-57.3**	-60.4	-61.4	-64.2	**-62**	-59.3	-60.1	-58.8	**-59.4**

Settleability analysis

Mass of S^{2-} added (mg/L)	**Settleability (mL/L)**			
	Run 1	Run 2	Run 3	Average
0	**6**	**7.5**	8.5	**7.3**
7	0	0	0	0
12	0	0	0	0

Appendix B

The zeta potential measurements of CuS particles, after Base-Acid and then Acid-Base pH titrations.

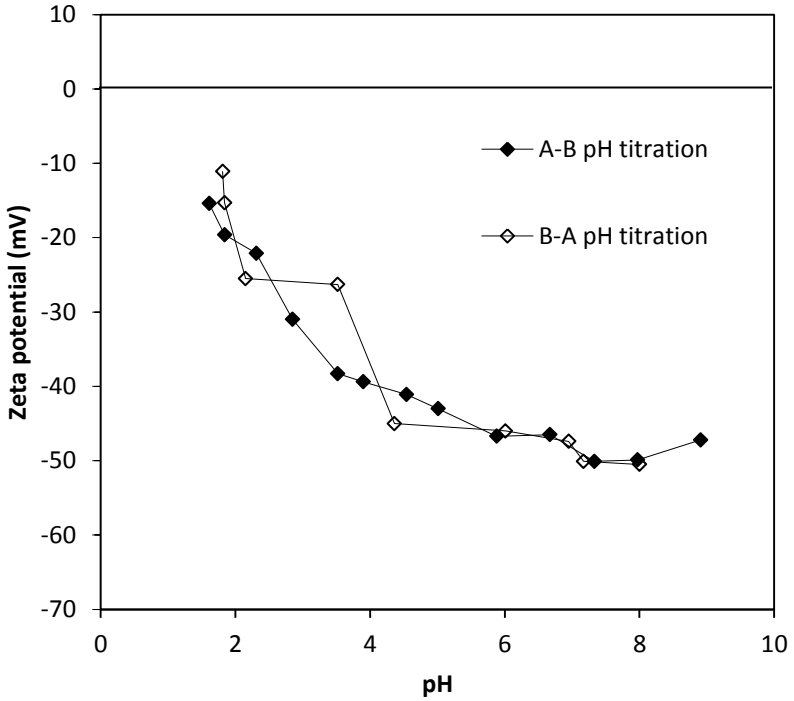

Appendix C

Raw data of zeta potential pH curves

0 minutes oxidation					
Run 1		Run 2		Run 3	
pH	Zeta Potential (mV)	pH	Zeta Potential (mV)	pH	Zeta Potential (mV)
1.61	-8.46	1.62	-8.23	1.61	-15.4
2.14	-20.4	2.05	-12.1	1.84	-19.6
2.62	-25.5	2.61	-19	2.31	-22.1
3.08	-31.2	3.16	-25.7	2.85	-31
3.58	-38.3	3.6	-27.6	3.52	-38.3
4.15	-40.5	4.12	-33.3	3.9	-39.4
4.46	-48.5	4.64	-35.1	4.54	-41.1
4.79	-51.1	4.83	-34.4	5.01	-43
5.73	-46.5	5.37	-39.6	5.88	-46.7
6.81	-45	5.88	-32.4	6.67	-46.5
7.31	-45.3	6.1	-29.2	7.33	-50.1
7.17	-40.5	7.07	-36.8	7.97	-49.9
				8.91	-47.2

30 minutes oxidation					
Run 1		Run 2		Run 3	
pH	Zeta Potential (mV)	pH	Zeta Potential (mV)	pH	Zeta Potential (mV)
1.64	-3.98	1.57	-1.51	8.08	-0.653
1.94	-3.96	1.94	-2.67	7.27	2.57
2.39	-3.69	2.42	-2.83	7.08	-3.63
2.89	-7.91	2.9	-6.04	6.42	-13.7
3.43	-10.7	3.43	-2.6	5.85	-18.3
3.9	-14.5	3.9	-15.8	5.05	-17.1
4.47	-22.4	4.47	-21.2	4.86	-19.9
5.01	-20.9	4.96	-20.2	4.63	-18.5
5.49	-23.1	5.51	-22.8	4.05	-20.5
5.96	-24	5.98	-28.5	3.57	-9.85
6.41	-25	6.43	-27.8	3.1	-12.6
6.89	-2.22	6.89	-12.4	2.62	-6.62
7.35	1.94	7.49	-0.842	2.12	-2.46
8.1	-2.34	7.83	-2.7	1.59	-0.288

60 minutes oxidation					
Run 1		Run 2		Run 3	
pH	Zeta Potential (mV)	pH	Zeta Potential (mV)	pH	Zeta Potential (mV)
1.64	-10.5	1.62	-7.5	1.61	-11.8
2.05	-10.7	2.08	-8.64	2.07	-6.83
2.41	-9.44	2.57	-13.4	2.57	-12.8
2.92	-8.67	3.11	-16.3	3.12	-18.8
3.46	-8.91	3.59	-21	3.61	-13
3.98	-13.7	4.01	-18.1	4.03	-10.8
4.62	-14.4	4.62	-17.9	4.41	-11.8
4.95	-16.8	4.95	-18	5.04	-16
5.47	-23.4	5.33	-16.1	5.26	-10.5
5.98	-17.8	5.58	-24.2	6.04	-14.8
6.38	-17.5	6.13	-15.3	6.57	-6.26
6.85	-3.12	7.81	-12.3	7.81	-0.01
7.49	0.361				
8.19	-0.86				

Appendix D-1

Phreeqc input code for CuS particles at 0 min oxidation

```
SOLUTION 1
pH 1.6
pe 1.69
units mmol/L
K 10
N(+5) 1 charge
END
SURFACE_MASTER_SPECIES
Cus_i Cus_iS-1.9947
Cus_v Cus_vS-0.0209
SURFACE 1
-equilibrate 1
-sites     DENSITY
Cus_iS-1.9947 9.8300E+000 1.3300E+002 7.5700E-001
Cus_vS-0.0209 9.8300E+000 1.3300E+002 7.5700E-001
-cd_music
-capacitance  0.3400 0.3400
SURFACE_SPECIES
Cus_iS-1.9947 = Cus_iS-1.9947
log_k 0.0
-cd_music 0 0 0 0 0
Cus_iS-1.9947 + H+ = Cus_iSH-0.9947
log_k 10.0000
-cd_music 1 0 0 0 0
Cus_iSH-0.9947 + H+ = Cus_iSH2+0.0053
log_k -1.2100
-cd_music 1 0 0 0 0
Cus_vS-0.0209 = Cus_vS-0.0209
log_k 0.0
-cd_music 0 0 0 0 0
Cus_vS-0.0209 + H+ = Cus_vSH+0.9791
log_k 7.4000
-cd_music 1 0 0 0 0
Cus_vSH+0.9791 + H+ = Cus_vSH2+1.9791
log_k -10.0000
-cd_music 1 0 0 0 0
END
SELECTED_OUTPUT
-reset false
USER_PUNCH
-headings pH zeta_potential
-start
10 punch -la("H+")
20 punch edl("psi2", "Cus")  * 1000
-end
END
USE SOLUTION 1
USE SURFACE 1
EQUILIBRIUM_PHASES 1-10
fix_H+ -1.6155 NaOH 0.1
END
USE SOLUTION 1
USE SURFACE 1
EQUILIBRIUM_PHASES 1-10
fix_H+ -1.6189 NaOH 0.1
END
USE SOLUTION 1
USE SURFACE 1
EQUILIBRIUM_PHASES 1-10
fix_H+ -1.8349 NaOH 0.1
END
USE SOLUTION 1
USE SURFACE 1
EQUILIBRIUM_PHASES 1-10
fix_H+ -2.1565 NaOH 0.1
END
USE SOLUTION 1
USE SURFACE 1
EQUILIBRIUM_PHASES 1-10
fix_H+ -2.3001 NaOH 0.1
END
USE SOLUTION 1
USE SURFACE 1
EQUILIBRIUM_PHASES 1-10
fix_H+ -2.6229 NaOH 0.1
END
USE SOLUTION 1
USE SURFACE 1
EQUILIBRIUM_PHASES 1-10
fix_H+ -2.8398 NaOH 0.1
END
USE SOLUTION 1
USE SURFACE 1
EQUILIBRIUM_PHASES 1-10
fix_H+ -3.0898 NaOH 0.1
END
USE SOLUTION 1
USE SURFACE 1
EQUILIBRIUM_PHASES 1-10
fix_H+ -3.5215 NaOH 0.1
END
USE SOLUTION 1
USE SURFACE 1
EQUILIBRIUM_PHASES 1-10
fix_H+ -3.5215 NaOH 0.1
END
USE SOLUTION 1
USE SURFACE 1
EQUILIBRIUM_PHASES 1-10
fix_H+ -3.9148 NaOH 0.1
END
USE SOLUTION 1
USE SURFACE 1
EQUILIBRIUM_PHASES 1-10
fix_H+ -4.1652 NaOH 0.1
END
USE SOLUTION 1
USE SURFACE 1
EQUILIBRIUM_PHASES 1-10
fix_H+ -4.5585 NaOH 0.1
END
USE SOLUTION 1
USE SURFACE 1
EQUILIBRIUM_PHASES 1-10
fix_H+ -5.0594 NaOH 0.1
END
USE SOLUTION 1
USE SURFACE 1
EQUILIBRIUM_PHASES 1-10
fix_H+ -5.7394 NaOH 0.1
END
USE SOLUTION 1
USE SURFACE 1
EQUILIBRIUM_PHASES 1-10
fix_H+ -5.8824 NaOH 0.1
END
```

```
USE SOLUTION 1
USE SURFACE 1
EQUILIBRIUM_PHASES 1-10
fix_H+ -7.3125 NaOH 0.1
END
USE SOLUTION 1
USE SURFACE 1
EQUILIBRIUM_PHASES 1-10
fix_H+ -7.9551 NaOH 0.1
END
```

Appendix D-2

Phreeqc input code for CuS particles oxidised for 30 min (low pH range)

```
SOLUTION 1
pH 1.6
pe 1.69
units mmol/L
K 10
N(+5) 1 charge
END
SURFACE_MASTER_SPECIES
Cus_i Cus_iS-1.9947
Cus_v Cus_vS-0.0209
Cus_j Cus_jO-1.9979
Cus_w Cus_wO-0.0737
SURFACE 1
-equilibrate 1
-sites     DENSITY
Cus_iS-1.9947 9.6712E+000 1.3300E+002 7.5700E-001
Cus_vS-0.0209 9.2999E+000 1.3300E+002 7.5700E-001
Cus_jO-1.9979 1.5880E-001 1.3300E+002 7.5700E-001
Cus_wO-0.0737 5.3010E-001 1.3300E+002 7.5700E-001
-cd_music
-capacitance  0.3400 0.3400
SURFACE_SPECIES
Cus_iS-1.9947 = Cus_iS-1.9947
log_k 0.0
-cd_music 0 0 0 0 0
Cus_iS-1.9947 + H+ = Cus_iSH-0.9947
log_k 10.0000
-cd_music 1 0 0 0 0
Cus_iSH-0.9947 + H+ = Cus_iSH2+0.0053
log_k -1.2100
-cd_music 1 0 0 0 0
Cus_vS-0.0209 = Cus_vS-0.0209
log_k 0.0
-cd_music 0 0 0 0 0
Cus_vS-0.0209 + H+ = Cus_vSH+0.9791
log_k 7.4000
-cd_music 1 0 0 0 0
Cus_vSH+0.9791 + H+ = Cus_vSH2+1.9791
log_k -10.0000
-cd_music 1 0 0 0 0
Cus_jO-1.9979 = Cus_jO-1.9979
log_k 0.0
-cd_music 0 0 0 0 0
Cus_jO-1.9979 + H+ = Cus_jOH-0.9979
log_k 9.5000
-cd_music 1 0 0 0 0
Cus_jOH-0.9979 + H+ = Cus_jOH2+0.0021
log_k 4.3057
-cd_music 1 0 0 0 0
Cus_wO-0.0737 = Cus_wO-0.0737
log_k 0.0
-cd_music 0 0 0 0 0
Cus_wO-0.0737 + H+ = Cus_wOH+0.9263
log_k 9.4995
-cd_music 1 0 0 0 0
Cus_wOH+0.9263 + H+ = Cus_wOH2+1.9263
log_k -10.0000
-cd_music 1 0 0 0 0
END
USER_GRAPH
-headings pH Calc_pZ_mV
-chart_title "Surface charge"
-axis_scale x_axis 2 9 1
-axis_scale y_axis  -0.30 0.30 0.050
-axis_scale sy_axis  -0.5 0.5 0.1
-axis_titles   "pH"      "pZ mV"      "Eh"
-initial_solutions false
-connect_simulations true
-start
10 graph_x -la("H+")
30 graph_y edl("psi2", "Cus")  * 1000
#40 graph_sy  -la("e-")/16.9
END
PHASES
Fix_H+
H+ = H+
log_k  0.0
END
USE SOLUTION 1
USE SURFACE 1
EQUILIBRIUM_PHASES 1-10
fix_H+ -1.6100 NaOH 0.1
END
USE SOLUTION 1
USE SURFACE 1
EQUILIBRIUM_PHASES 1-10
fix_H+ -1.6100 NaOH 0.1
END
USE SOLUTION 1
USE SURFACE 1
EQUILIBRIUM_PHASES 1-10
fix_H+ -1.6800 NaOH 0.1
END
USE SOLUTION 1
USE SURFACE 1
EQUILIBRIUM_PHASES 1-10
fix_H+ -1.9300 NaOH 0.1
END
USE SOLUTION 1
USE SURFACE 1
EQUILIBRIUM_PHASES 1-10
fix_H+ -1.9300 NaOH 0.1
END
USE SOLUTION 1
USE SURFACE 1
EQUILIBRIUM_PHASES 1-10
fix_H+ -2.1100 NaOH 0.1
END
USE SOLUTION 1
USE SURFACE 1
EQUILIBRIUM_PHASES 1-10
fix_H+ -2.4000 NaOH 0.1
END
USE SOLUTION 1
USE SURFACE 1
EQUILIBRIUM_PHASES 1-10
fix_H+ -2.4700 NaOH 0.1
END
USE SOLUTION 1
USE SURFACE 1
EQUILIBRIUM_PHASES 1-10
fix_H+ -2.6100 NaOH 0.1
END
USE SOLUTION 1
```

```
USE SURFACE 1
EQUILIBRIUM_PHASES 1-10
fix_H+ -2.9000 NaOH 0.1
END
USE SOLUTION 1
USE SURFACE 1
EQUILIBRIUM_PHASES 1-10
fix_H+ -2.9300 NaOH 0.1
END
USE SOLUTION 1
USE SURFACE 1
EQUILIBRIUM_PHASES 1-10
fix_H+ -3.1400 NaOH 0.1
END
USE SOLUTION 1
USE SURFACE 1
EQUILIBRIUM_PHASES 1-10
fix_H+ -3.4700 NaOH 0.1
END
USE SOLUTION 1
USE SURFACE 1
EQUILIBRIUM_PHASES 1-10
fix_H+ -3.4700 NaOH 0.1
END
USE SOLUTION 1
USE SURFACE 1
EQUILIBRIUM_PHASES 1-10
fix_H+ -3.6100 NaOH 0.1
END
USE SOLUTION 1
USE SURFACE 1
EQUILIBRIUM_PHASES 1-10
fix_H+ -3.8900 NaOH 0.1
END
USE SOLUTION 1
USE SURFACE 1
EQUILIBRIUM_PHASES 1-10
fix_H+ -3.9300 NaOH 0.1
END
USE SOLUTION 1
USE SURFACE 1
EQUILIBRIUM_PHASES 1-10
fix_H+ -4.0700 NaOH 0.1
END
USE SOLUTION 1
USE SURFACE 1
EQUILIBRIUM_PHASES 1-10
fix_H+ -4.4700 NaOH 0.1
END
USE SOLUTION 1
USE SURFACE 1
EQUILIBRIUM_PHASES 1-10
fix_H+ -4.5000 NaOH 0.1
END
USE SOLUTION 1
USE SURFACE 1
EQUILIBRIUM_PHASES 1-10
fix_H+ -4.6500 NaOH 0.1
END
USE SOLUTION 1
USE SURFACE 1
EQUILIBRIUM_PHASES 1-10
fix_H+ -5.0000 NaOH 0.1
END
USE SOLUTION 1
USE SURFACE 1
EQUILIBRIUM_PHASES 1-10
fix_H+ -5.0400 NaOH 0.1
END
USE SOLUTION 1
USE SURFACE 1
EQUILIBRIUM_PHASES 1-10
fix_H+ -5.0800 NaOH 0.1
END
USE SOLUTION 1
USE SURFACE 1
EQUILIBRIUM_PHASES 1-10
fix_H+ -5.5400 NaOH 0.1
END
USE SOLUTION 1
USE SURFACE 1
EQUILIBRIUM_PHASES 1-10
fix_H+ -5.8700 NaOH 0.1
END
USE SOLUTION 1
USE SURFACE 1
EQUILIBRIUM_PHASES 1-10
fix_H+ -5.9700 NaOH 0.1
END
USE SOLUTION 1
USE SURFACE 1
EQUILIBRIUM_PHASES 1-10
fix_H+ -6.0100 NaOH 0.1
END
```

Appendix D-3

Phreeqc input code for CuS particles oxidised for 30 min (full pH range)

```
SOLUTION 1
pH 1.6
pe 1.69
units mmol/L
K 10
N(+5) 1 charge
Cu 2.7000E-001
END
SURFACE_MASTER_SPECIES
Cus_i Cus_iS-1.9947
Cus_v Cus_vS-0.0209
Cus_j Cus_jO-1.9979
Cus_w Cus_wO-0.0737
SURFACE 1
-equilibrate 1
-sites     DENSITY
Cus_iS-1.9947 9.6712E+000 1.3300E+002 7.5700E-001
Cus_vS-0.0209 9.2999E+000 1.3300E+002 7.5700E-001
Cus_jO-1.9979 1.5880E-001 1.3300E+002 7.5700E-001
Cus_wO-0.0737 5.3010E-001 1.3300E+002 7.5700E-001
-cd_music
-capacitance  0.3400 0.3400
SURFACE_SPECIES
Cus_iS-1.9947 = Cus_iS-1.9947
log_k 0.0
-cd_music 0 0 0 0 0
Cus_iS-1.9947 + H+ = Cus_iSH-0.9947
log_k 10.0000
-cd_music 1 0 0 0 0
Cus_iSH-0.9947 + H+ = Cus_iSH2+0.0053
log_k -1.2100
-cd_music 1 0 0 0 0
Cus_iSH-0.9947 + CuOH+1.0000 = Cus_iSHCuOH+0.0053
log_k 2.3599
-cd_music 0 0 1.0000 0 0
Cus_vS-0.0209 = Cus_vS-0.0209
log_k 0.0
-cd_music 0 0 0 0 0
Cus_vS-0.0209 + H+ = Cus_vSH+0.9791
log_k 7.4000
-cd_music 1 0 0 0 0
Cus_vSH+0.9791 + H+ = Cus_vSH2+1.9791
log_k -10.0000
-cd_music 1 0 0 0 0
Cus_vSH+0.9791 + CuOH+1.0000 = Cus_vSHCuOH+1.9791
log_k 2.3045
-cd_music 0 0 1.0000 0 0
Cus_jO-1.9979 = Cus_jO-1.9979
log_k 0.0
-cd_music 0 0 0 0 0
Cus_jO-1.9979 + H+ = Cus_jOH-0.9979
log_k 9.5000
-cd_music 1 0 0 0 0
Cus_jOH-0.9979 + H+ = Cus_jOH2+0.0021
log_k 4.3057
-cd_music 1 0 0 0 0
Cus_jOH-0.9979 + CuOH+1.0000 = Cus_jOHCuOH+0.0021
log_k 3.1273
-cd_music 0 0 1.0000 0 0
Cus_wO-0.0737 = Cus_wO-0.0737
log_k 0.0
-cd_music 0 0 0 0 0
Cus_wO-0.0737 + H+ = Cus_wOH+0.9263
log_k 9.4995
-cd_music 1 0 0 0 0
Cus_wOH+0.9263 + H+ = Cus_wOH2+1.9263
log_k -10.0000
-cd_music 1 0 0 0 0
Cus_wOH+0.9263 + CuOH+1.0000 = Cus_wOHCuOH+1.9263
log_k 2.3649
-cd_music 0 0 1.0000 0 0
END
USER_GRAPH
-headings pH Calc_pZ_mV
-chart_title "Surface charge"
-axis_scale x_axis 2 9 1
-axis_scale y_axis  -0.30 0.30 0.050
-axis_scale sy_axis  -0.5 0.5 0.1
-axis_titles   "pH"       "pZ mV"       "Eh"
-initial_solutions false
-connect_simulations true
-start
10 graph_x -la("H+")
30 graph_y edl("psi2", "Cus")  * 1000
#40 graph_sy  -la("e-")/16.9
END
PHASES
Fix_H+
H+ = H+
log_k  0.0
END
USE SOLUTION 1
USE SURFACE 1
EQUILIBRIUM_PHASES 1-10
fix_H+ -1.6100 NaOH 0.1
END
USE SOLUTION 1
USE SURFACE 1
EQUILIBRIUM_PHASES 1-10
fix_H+ -1.6100 NaOH 0.1
END
USE SOLUTION 1
USE SURFACE 1
EQUILIBRIUM_PHASES 1-10
fix_H+ -1.6800 NaOH 0.1
END
USE SOLUTION 1
USE SURFACE 1
EQUILIBRIUM_PHASES 1-10
fix_H+ -1.9300 NaOH 0.1
END
USE SOLUTION 1
USE SURFACE 1
EQUILIBRIUM_PHASES 1-10
fix_H+ -1.9300 NaOH 0.1
END
USE SOLUTION 1
USE SURFACE 1
EQUILIBRIUM_PHASES 1-10
fix_H+ -2.1100 NaOH 0.1
END
USE SOLUTION 1
USE SURFACE 1
EQUILIBRIUM_PHASES 1-10
```

```
fix_H+ -2.4000 NaOH 0.1
END
USE SOLUTION 1
USE SURFACE 1
EQUILIBRIUM_PHASES 1-10
fix_H+ -2.4700 NaOH 0.1
END
USE SOLUTION 1
USE SURFACE 1
EQUILIBRIUM_PHASES 1-10
fix_H+ -2.6100 NaOH 0.1
END
USE SOLUTION 1
USE SURFACE 1
EQUILIBRIUM_PHASES 1-10
fix_H+ -2.9000 NaOH 0.1
END
USE SOLUTION 1
USE SURFACE 1
EQUILIBRIUM_PHASES 1-10
fix_H+ -2.9300 NaOH 0.1
END
USE SOLUTION 1
USE SURFACE 1
EQUILIBRIUM_PHASES 1-10
fix_H+ -3.1400 NaOH 0.1
END
USE SOLUTION 1
USE SURFACE 1
EQUILIBRIUM_PHASES 1-10
fix_H+ -3.4700 NaOH 0.1
END
USE SOLUTION 1
USE SURFACE 1
EQUILIBRIUM_PHASES 1-10
fix_H+ -3.4700 NaOH 0.1
END
USE SOLUTION 1
USE SURFACE 1
EQUILIBRIUM_PHASES 1-10
fix_H+ -3.6100 NaOH 0.1
END
USE SOLUTION 1
USE SURFACE 1
EQUILIBRIUM_PHASES 1-10
fix_H+ -3.8900 NaOH 0.1
END
USE SOLUTION 1
USE SURFACE 1
EQUILIBRIUM_PHASES 1-10
fix_H+ -3.9300 NaOH 0.1
END
USE SOLUTION 1
USE SURFACE 1
EQUILIBRIUM_PHASES 1-10
fix_H+ -4.0700 NaOH 0.1
END
USE SOLUTION 1
USE SURFACE 1
EQUILIBRIUM_PHASES 1-10
fix_H+ -4.4700 NaOH 0.1
END
USE SOLUTION 1
USE SURFACE 1
EQUILIBRIUM_PHASES 1-10
fix_H+ -4.5000 NaOH 0.1
END
USE SOLUTION 1
USE SURFACE 1
EQUILIBRIUM_PHASES 1-10
fix_H+ -4.6500 NaOH 0.1
END
USE SOLUTION 1
USE SURFACE 1
EQUILIBRIUM_PHASES 1-10
fix_H+ -5.0000 NaOH 0.1
END
USE SOLUTION 1
USE SURFACE 1
EQUILIBRIUM_PHASES 1-10
fix_H+ -5.0400 NaOH 0.1
END
USE SOLUTION 1
USE SURFACE 1
EQUILIBRIUM_PHASES 1-10
fix_H+ -5.0800 NaOH 0.1
END
USE SOLUTION 1
USE SURFACE 1
EQUILIBRIUM_PHASES 1-10
fix_H+ -5.5400 NaOH 0.1
END
USE SOLUTION 1
USE SURFACE 1
EQUILIBRIUM_PHASES 1-10
fix_H+ -5.8700 NaOH 0.1
END
USE SOLUTION 1
USE SURFACE 1
EQUILIBRIUM_PHASES 1-10
fix_H+ -5.9700 NaOH 0.1
END
USE SOLUTION 1
USE SURFACE 1
EQUILIBRIUM_PHASES 1-10
fix_H+ -6.0100 NaOH 0.1
END
USE SOLUTION 1
USE SURFACE 1
EQUILIBRIUM_PHASES 1-10
fix_H+ -6.4400 NaOH 0.1
END
USE SOLUTION 1
USE SURFACE 1
EQUILIBRIUM_PHASES 1-10
fix_H+ -6.4700 NaOH 0.1
END
USE SOLUTION 1
USE SURFACE 1
EQUILIBRIUM_PHASES 1-10
fix_H+ -6.4800 NaOH 0.1
END
USE SOLUTION 1
USE SURFACE 1
EQUILIBRIUM_PHASES 1-10
fix_H+ -6.9100 NaOH 0.1
END
USE SOLUTION 1
USE SURFACE 1
EQUILIBRIUM_PHASES 1-10
fix_H+ -6.9500 NaOH 0.1
END
USE SOLUTION 1
USE SURFACE 1
EQUILIBRIUM_PHASES 1-10
fix_H+ -7.1300 NaOH 0.1
END
USE SOLUTION 1
USE SURFACE 1
EQUILIBRIUM_PHASES 1-10
```

```
fix_H+ -7.2700 NaOH 0.1
END
USE SOLUTION 1
USE SURFACE 1
EQUILIBRIUM_PHASES 1-10
fix_H+ -7.3800 NaOH 0.1
END
USE SOLUTION 1
USE SURFACE 1
EQUILIBRIUM_PHASES 1-10
fix_H+ -7.4900 NaOH 0.1
END
USE SOLUTION 1
USE SURFACE 1
EQUILIBRIUM_PHASES 1-10
fix_H+ -7.8400 NaOH 0.1
END
USE SOLUTION 1
USE SURFACE 1
EQUILIBRIUM_PHASES 1-10
fix_H+ -8.1300 NaOH 0.1
END
USE SOLUTION 1
USE SURFACE 1
EQUILIBRIUM_PHASES 1-10
fix_H+ -8.1700 NaOH 0.1
END
```